



**UNIVERSIDAD NACIONAL AUTÓNOMA DE MÉXICO
POSGRADO EN CIENCIA E INGENIERÍA DE LA COMPUTACIÓN**

**“AUGMENTED REALITY SURGICAL NAVIGATION AS TRAINING
MODEL IN NEUROSURGERY: VENTRICULOSTOMY PROCEDURES”**

TESIS

**QUE PARA OPTAR POR EL GRADO DE
DOCTOR EN CIENCIA E INGENIERÍA DE LA COMPUTACIÓN**

PRESENTA

CÉSAR FABIÁN DOMÍNGUEZ VELASCO

TUTOR

DR. MIGUEL ÁNGEL PADILLA CASTAÑEDA

INSTITUTO DE CIENCIAS APLICADAS Y TECNOLOGÍA

CIUDAD UNIVERSITARIA, CD. MX., OCTUBRE DE 2023.



Universidad Nacional
Autónoma de México



UNAM – Dirección General de Bibliotecas
Tesis Digitales
Restricciones de uso

DERECHOS RESERVADOS ©
PROHIBIDA SU REPRODUCCIÓN TOTAL O PARCIAL

Todo el material contenido en esta tesis esta protegido por la Ley Federal del Derecho de Autor (LFDA) de los Estados Unidos Mexicanos (México).

El uso de imágenes, fragmentos de videos, y demás material que sea objeto de protección de los derechos de autor, será exclusivamente para fines educativos e informativos y deberá citar la fuente donde la obtuvo mencionando el autor o autores. Cualquier uso distinto como el lucro, reproducción, edición o modificación, será perseguido y sancionado por el respectivo titular de los Derechos de Autor.

ACKNOWLEDGEMENTS

To the Postgraduate in Computer Science and Engineering and the administrative staff, for all the facilities they gave me in carrying out this work.

I am grateful to CONAHCyT for financing me with a doctoral studies scholarship.

To my thesis director, Dr. Miguel Ángel Padilla Castañeda, for all his friendship, time, patience, support, and teachings. For having guided me through this process with such dedication and commitment.

To Professor Vincenzo Ferrari of the University of Pisa, for the opportunity to carry out my stay in his research group in Italy and for his valuable guidance as an evaluator.

To Dr. Isaac Tello Mata of the National Institute of Neurology and Neurosurgery “Dr. Manuel Velasco Suárez”, for his guidance and collaboration in this work.

To my mother Noemí and my sister Viridiana for their love, support, and unconditional trust.

To my life partner Alexandra, for her unconditional support during my studies.

To my children Valeria and Mateo, for being my daily motivation and strength.

To my colleagues and friends for their support and motivation.

I want to thank the projects **“Esquema de neuronavegación quirúrgica por imágenes multiespectrales y simulación biomecánica para resección de tumores cerebrales guiada por computadora”** DGAPA-PAPIIT TA101422, **“Metodología de realidad aumentada multiespectral para la identificación y localización de tejido patológico en intervenciones quirúrgicas guiadas por computadora”** CONAHCyT 319585, **SECTEI 219/2019**, and **SECTEI 087/2023 “Laboratorio de Investigación y Desarrollo de Simuladores Clínicos y Cirugía Asistida por Computadora”** for financing this work.

SUMMARY

Background: Ventricular puncture is a common procedure in neurosurgery and the first that residents must learn. Ongoing education is critical to improve patient outcomes. However, training at the expense of potential risk to patients warrants new and safer training methods for residents.

Methods: An augmented reality (AR) simulator for the practice of ventricular punctures was designed. It consists of a navigation system with a virtual 3D projection of the anatomy over a 3D-printed patient model. Forty-eight participants from neurosurgery staff performed two free-hand ventricular punctures before and after a training session.

Results: After practicing with the system, participants achieved enhanced accuracy in reaching the target at the Monro foramen. Additional metrics revealed significantly better trajectories after the training.

Conclusion: The study confirms the feasibility of AR as a training tool. It motivates future work toward standardizing new educative methodologies in neurosurgery.

Keywords: Augmented Reality, Surgery Simulation, Surgery training, Patient-specific printed models, Neurosurgery, Ventriculostomy

LIST OF PUBLICATIONS

International Journals

1. **Domínguez-Velasco, C. F.**, Tello-Mata, I. E., Guinto-Nishimura, G., Martínez-Hernández, A., Alcocer-Barradas, V., Pérez-Lomelí, J. S., & Padilla-Castañeda, M. A. (2023). Augmented reality simulation as training model of ventricular puncture: Evidence in the improvement of the quality of punctures. *The International Journal of Medical Robotics and Computer Assisted Surgery*, e2529.
2. De Paolis, L. T., Vite, S. T., Castañeda, M. Á. P., **Dominguez Velasco, C. F.**, Muscatello, S., & Hernández Valencia, A. F. (2022). An augmented reality platform with hand gestures-based navigation for applications in image-guided surgery: prospective concept evaluation by surgeons. *International Journal of Human-Computer Interaction*, 38(2), 131-143.
3. Teodoro-Vite, S., Pérez-Lomelí, J. S., **Domínguez-Velasco, C. F.**, Hernández-Valencia, A. F., Capurso-García, M. A., & Padilla-Castañeda, M. A. (2021). A high-fidelity hybrid virtual reality simulator of aneurysm clipping repair with brain sylvian fissure exploration for vascular neurosurgery training. *Simulation in Healthcare*, 16(4), 285-294.

International Conferences/Workshops with Peer Review

1. **C.F. Domínguez-Velasco**, J.S. Pérez-Lomelí, M.A. Padilla-Castañeda*, I. E. Tello-Mata and V. Alcocer-Barradas, "A Ventriculostomy Simulation through Augmented Reality Navigation System for Learning and Improving Skills in Neurosurgery," 2022 IEEE Mexican International Conference on Computer Science (ENC), 2022, pp. 1-3, doi: 10.1109/ENC56672.2022.9882933.
2. S. Teodoro-Vite, I. Tello, **C.F. Domínguez-Velasco**, J. Alatorre, J.S. Pérez-Lomelí, V. Alcocer-Barradas, M.A. Padilla-Castañeda. An Augmented Reality Based Application with Haptic Feedback for Ventricular Puncture Procedures in Neurosurgery. EuroVR 2019, October 23-25, 2019. Tallin, Estonia.

3. **Domínguez Velasco C.F.**, Pérez Lomelí J.S., Padilla Castañeda M.A., Tello Mata I.E., Alcocer Barradas V. Simulación virtual de punción ventricular: Un enfoque hacia el desarrollo y perfeccionamiento de habilidades neuroquirúrgicas. Sexto Encuentro Int. de Simulación Clínica SIMex 2022. Cd. Mx. 16-18 noviembre, 2022
4. **C.F. Domínguez-Velasco**, I. E. Tello-Mata, V. Alcocer-Barradas, J.S. Pérez-Lomelí y M.A. Padilla-Castañeda. Modelo de entrenamiento de simulación con realidad aumentada para procedimientos de punción ventricular neuroquirúrgica. XII Congreso Nacional de Tecnología Aplicada a Ciencias de la Salud, XII CONTACTS. Puebla, Puebla, 9-11 junio, 2022.
5. **C.F. Domínguez-Velasco**, I.E. Tello-Mata, J.S. Pérez-Lomelí, V. Alcocer-Barradas, M.A. Padilla-Castañeda. Simulador híbrido para entrenamiento en procedimientos de ventriculostomía combinando realidad virtual y modelos de impresión 3D. Cuarto Encuentro Int. de Simulación Clínica SIMex 2020. Cd. Mx. 18-19 noviembre, 2020.

Patent Pending

1. M.A. Padilla Castañeda; J.S. Pérez Lomelí; S. Teodoro Vite; **C.F. Domínguez Velasco**; D. Vargas Castro; L.A. Morales Bautista; L.M. Vidal Flores. “Simulador para procedimientos de neurocirugía combinando realidad virtual y modelos anatómicos”, Tipo de registro: Patente. Expediente MX/a/2021/008243, Solicitud 72563. País: México.

Industrial Models

1. J.S. Pérez Lomelí; M.A. Padilla Castañeda; S. Teodoro Vite; **C.F. Domínguez Velasco**, “Modelo Industrial de una estación de trabajo de simulador híbrido por realidad virtual para entrenamiento en neurocirugía”, Tipo de registro: Modelo Industrial. Expediente MX/f/2021/001497, Solicitud 81417. País: México.

Software Copyright

1. **C.F. Domínguez Velasco**, J. Alatorre Flores, M.A. Padilla Castañeda, J.S. Pérez Lomelí. (2022). BACSIM Ventricular AR Simulator Software. Tipo de registro: Derechos de autor de Software. Status: pending.
2. I.A. Gutiérrez Giles, **C.F. Domínguez Velasco**, D. Vargas Castro, M.A. Padilla Castañeda. (2022). BACSIM Haptic Ventriculostomy VR Software. Tipo de registro: Derechos de autor de Software. Status: pending.

User validated Prototypes

1. Iván A. Gutiérrez Giles, **César F. Domínguez Velasco**, Juan S. Pérez Lomelí, Miguel A. Padilla Castañeda. Simulador por realidad virtual y retroalimentación háptica de navegación neuroendoscópica. Usuario: Unidad Neurocirugía, Instituto Nacional de Neurología y Neurocirugía Dr. Manuel Velasco. (2022)
2. J.S. Pérez Lomelí, L.M. Vidal Flores, **C.F. Domínguez Velasco**, M.A. Padilla-Castañeda. Modelo anatómico de simulación de resección y disección de membranas cerebrales. Usuario: Unidad Neurocirugía, Instituto Nacional de Neurología y Neurocirugía Dr. Manuel Velasco. (2021)
3. **C.F. Domínguez Velasco**, J.S. Pérez Lomelí, M.A. Padilla-Castañeda. Simulador de punción ventricular por realidad aumentada y modelos anatómicos. Versión 1. Usuario: Unidad Neurocirugía, Instituto Nacional de Neurología y Neurocirugía Dr. Manuel Velasco. (2021).

TABLE OF CONTENTS

ACKNOWLEDGEMENTS	I
SUMMARY	II
LIST OF PUBLICATIONS	III
CHAPTER 1 INTRODUCTION	1
1.1. TECHNOLOGICAL FOUNDATIONS	1
1.1.1. <i>AUGMENTED REALITY</i>	2
1.1.2. <i>CALIBRATION</i>	3
1.1.3. <i>3D PRINTING IN SIMULATION</i>	4
1.2. AUGMENTED REALITY IN NEUROSURGERY	4
1.3. NAVIGATION FOR SURGICAL PROCEDURES OF THE BRAIN	5
CHAPTER 2 SIMULATION IN NEUROSURGERY: TECHNOLOGICAL APPROACHES FOR THE ANALYSIS OF THE IMPROVEMENT OF SKILLS IN VENTRICULOSTOMY	7
2.1. RELATED WORK	10
2.1.1. <i>VENTROAR</i>	10
2.1.2. <i>AUGMENTED REALITY-ASSISTED VENTRICULOSTOMY</i>	11
2.1.3. <i>HOLOQUICKNAV</i>	12
CHAPTER 3 INTEGRATION OF A PATIENT MODEL TO AN AUGMENTED REALITY NAVIGATION SYSTEM	15
3.1. THE PATIENT MODEL	15
3.2. THE AUGMENTED REALITY SIMULATOR.....	18
CHAPTER 4 ACCURACY MEASUREMENT AND TESTING	22
4.1. CAMERA CALIBRATION	22
4.2. HAND-EYE CALIBRATION (AXXB)	24
4.3. SINGULAR VALUE DECOMPOSITION (SVD)	27
4.4. SYSTEM ERROR MEASUREMENT	31

CHAPTER 5 AUGMENTED REALITY NAVIGATION FOR VENTRICULAR PUNCTURE: EXPERIMENTS	33
5.1. THE OBJECTIVE OF THE STUDY	33
5.2. PARTICIPANTS	33
5.3. EXPERIMENTAL PROCEDURE	33
5.4. MEASUREMENTS.....	35
5.5. STATISTICAL ANALYSIS.....	36
5.6. COMPARISON BETWEEN VENTRICULAR PUNCTURE SYSTEMS.....	36
CHAPTER 6 RESULTS	40
CHAPTER 7 DISCUSSION	48
CHAPTER 8 CONCLUSION	54
BIBLIOGRAPHY.....	56

CHAPTER 1

INTRODUCTION

This chapter provides the basic concepts that surround this doctoral work, within which concepts such as augmented reality are introduced since it is one of the basic technologies of this work.

On the other hand, emphasis is placed on the principles of neuronavigation since they are computational technologies that support the surgeon to have a guide inside the human skull. This topic describes marker-based tracking technology.

Finally, an application based on augmented reality is proposed in combination with the bases of neuronavigation which can provide the neurosurgeon with a map of the cerebral ventricular system, as well as visual guides for the improvement of the quality of a puncture. The system superimposes on the patient the skull and the ventricles, which come from computed tomography studies.

1.1. TECHNOLOGICAL FOUNDATIONS

In neurosurgery interventions, in addition to the standardized procedures performed by specialists, computed tomography has been adopted as visual support. These layered images allow the physician to plan and discuss approaches with others responsible for surgery. During the intervention, it is common for more images to be requested to confirm the status of the procedure, even after surgery.

The use of computed tomography has become one of the tools to be able to diagnose patients, in such a way that those conditions that require an invasive operation to generate a diagnosis can now be determined by radiology because it is a non-invasive

test. On the other hand, studies (Redberg, 2009) have been carried out where it has been promoted that exposure to high doses of radiation from scans translates into the possibility of developing cancer. It is essential that with the increased use of CT scans, clinicians take radiation risks into account when testing their patients.

Thanks to the fact that virtual reality and augmented reality technologies have matured in the field of education combined with the field of surgery, it is possible to provide the clinician with more detailed information, as well as improve safety and reduce risks (Huang et al., 2018). In the areas of neurosurgery, these technologies have been further developed, to the point that the physician can use HMD to combine patient-specific medical information and CT images.

1.1.1. AUGMENTED REALITY

In the area of medicine, an augmented reality application provides the clinician with computer-processed image data in real-time through dedicated hardware and software. Augmented reality projection is usually done through screens, cameras, or projectors. A computer graphics image is superimposed on a real-world image captured by a camera and the combination of these is displayed on a computer, tablet, or projector (Vávra et al., 2017).

The applications of augmented reality in surgical interventions are required to make use of the images of tomography studies of the patient, from which 3D reconstructions of anatomical structures can be generated. These reconstructions can be performed with specialized software, through the DICOM format.

An advantage of highlighting augmented reality and its use in surgical procedures on patients is the reduction of risks and intervention times. This is because planning work can be carried out before surgery, even fully replicating the entire procedure through simulation.

1.1.2. CALIBRATION

A requirement in augmented reality systems is the registration of virtual environments with real space. These systems are prone to visual misalignment and are more noticeable due to the sensitivity of our sense of sight. In this sense, registration can be done in different ways and is a subject under study in research currently under development. A calibration process must be performed to compensate for misalignments between the virtual and physical world models.

An augmented reality system is composed of virtual and real entities. Calibration is the process of using values as parameters so that computational objects match models of the real physical world. Those models can be optical properties of a physical camera, as well as the orientation and position information of entities such as the camera, optical trackers, and other objects.

To determine the calibration steps to perform, it is necessary to establish a complete mapping from the real world to the virtual world. In this sense, it is important to list and identify the various devices and coordinate systems present in the navigator.

There are devices such as the camera and the optical tracker that have intrinsic parameters that affect the result of an augmented image. In this case, the coordinate systems are related to each other through a set of rigid transformations. There must be a World Coordinate System, which must be known and be always fixed, relative to the workspace. During the execution of an augmented reality system, all the components must operate in a unified way in the work environment (Tuceryan et al., 1995).

The coordinate systems of an augmented reality system must be linked to each other, as well as the intrinsic parameters of any device. Some transformations are known through direct measurements from devices such as the optical tracker. Other transformations are determined by employing a calibration process. Finally, the missing transformations are inferred from the set of known transformations. Intrinsic properties of devices such as the camera, are determined through a

calibration procedure, where the focal length (distance between the pinhole and the image plane), the principal point offset (location of the projection of the line perpendicular to the plane of the image that passes through the pinhole, relative to the origin of the film) and the axis skew.

One of the primary goals of an augmented reality system is to fill in all the gaps in terms of unknown transformations.

1.1.3. 3D PRINTING IN SIMULATION

Technical developments in 3D printing for medicine have continuously evolved. The workflow for 3D printing integrates several sequential steps: 1) 3D data acquisition, 2) segmentation, 3) conversion of a DICOM format file to a 3D mesh format file, 4) computer-aided design (CAD), and 5) 3D printing. High-resolution 3D imaging data acquisition with excellent image quality is mandatory for the creation of quality 3D printed models (Goo et al., 2020).

One of the main advantages of performing operations on 3D-printed models is the possibility of replicating a surgical procedure on a reliable copy of a patient's anatomy. This practice technique has become popular in areas of medical education (Ganguli et al., 2018) since an educational model is promoted where there is practically no risk to a patient, lowering costs in hospitals and allowing repeatability and therefore a way in which students of medicine can complement their training.

1.2. AUGMENTED REALITY IN NEUROSURGERY

Research related to augmented reality systems in neurosurgery has had great growth because one of its objectives is the search for minimal invasion and maximizing safety for both the patient and the doctor. Augmented reality-based neuronavigation provides real-time information on anatomical details, in addition to being superimposed on the surgical work area.

In the state of the art, works related to augmented reality can be found, which can be classified by surgical techniques or by the materials of the procedure, such as the use

of microscopes, by the use of fixed cameras, or HMD, for direct visualization of the patient, endoscopy, based on tumors, neurovascular, hydrocephalus, among others (Meola et al., 2017).

1.3. NAVIGATION FOR SURGICAL PROCEDURES OF THE BRAIN

The principle of neuronavigation consists of having a map of the patient's brain, which is why techniques based on passive markers tracked by optical systems have been implemented. Markers are placed on the patient and a CT scan is performed. The result is a model of patient image slices where by palpating the physical markers with a probe, a record is made with the markers in the images. Studies carried out with neuronavigation systems report a root mean square error (RMSE) of 1.0 ± 0.07 mm in controlled laboratory tests and 3.08 ± 1.57 mm in clinical tests (Ecke et al., 2003). In an environment where minimal error in registration is required and consequently high precision for neurosurgical interventions, this methodology could be extrapolated for simulations in 3D printed models.

Today there are computer applications are being created that support both basic and highly specialized medical procedures. Thanks to this, hospital staff shortens the learning curve with the benefit of offering patients and themselves reduced risks, especially in surgery. Although the technology promises many benefits, the reality is that not all hospitals have access to these tools, mainly because of their cost or for very limited groups such as private hospitals or research groups.

In neurosurgery, there are many high-risk procedures that both residents and specialists perform on patients. This research aims to provide a tool for learning ventricular punctures since it is a task that residents of the area must learn at the beginning of the specialty. In conjunction with the National Institute of Neurology and Neurosurgery "Manuel Velasco Suárez" (INNN), the need was found to improve the understanding of the procedure and the success rate, since neurosurgeons use a standard technique where they consider craniometric points and the imaginary drawing of guidelines to perform a puncture. After that, the staff requests a

tomography to confirm the correct placement of a catheter within the patient's ventricular system. This brings a cascade of implications from ionizing energy exposure for the patient and staff, as well as the possibility of post-procedure complications for the patient.

In this work, a neuronavigation methodology oriented to specific education per patient is proposed, by obtaining ventricular and skull anatomical models, printing the skull, and creating a neuronavigator that allows measuring the quality of ventricular punctures through metrics. The puncture movements are tracked with the help of an optical tracker. This work is not intended to replace the learning that students receive through other more experienced specialists, but rather to complement their learning process.

CHAPTER 2

SIMULATION IN NEUROSURGERY: TECHNOLOGICAL APPROACHES FOR THE ANALYSIS OF THE IMPROVEMENT OF SKILLS IN VENTRICULOSTOMY

Simulation in the health area has increased in the last 25 years (Contreras López et al., 2019; Fiani et al., 2020), in medicine and its different specialty branches, the need to use these tools as a complementary teaching method to the traditional model (Desselle et al., 2020). The aforementioned is based on being able to offer patient care in a safe and professional environment (Loh et al., 2018; Zhalmukhamedov & Urakov, n.d.). For this reason, teaching methodologies have been proposed for the acquisition of surgical skills such as intervention in animals and cadaveric models, however, the latter implies high maintenance costs, and not all hospitals have cadavers available for practice. Alternatively, computer simulators have been created that reproduce the procedure and anatomical models similar to reality (Hvolbek et al., 2019); they also allow contextual and detailed pre-planning of medical procedures, postoperative collaborative review, and advanced remote interaction (Desselle et al., 2020).

More specifically in neurosurgery, simulation systems based on virtual reality (VR) and augmented reality (AR) have been created as training schemes that can compensate for aspects such as the low availability of operations in the operating room (related to the high population of students and the low occurrence of cases for a specific intervention), the acquisition of cadaveric material and consequently reduce costs associated with maintenance (Kashikar et al., 2019). Given that neurosurgery considers precision as one of the most important aspects of operations, virtual simulators can replicate a procedure while maintaining a precision very close to the real one. It is also possible to collect information

from the participant, to apply metrics to identify the time to complete a task, efficiency, movement economy, manual dexterity, and collisions, among others (Dubin et al., 2017).

Ventricular puncture is involved in some of the most common procedures in neurosurgery. The importance of performing an accurate puncture lies in the significant morbidity and mortality associated with a misplaced catheter. This has led to the search for new

technologies to guide a proper puncture, such as navigation systems, stereotaxy, and ultrasound (Sarrafzadeh et al., 2014). However, the free-hand technique is the most frequently used method in low-resource settings (Gilbert et al., 2009). With this method, only 56% of ventricular catheters are correctly positioned (Huyette et al., 2008).

A poorly placed catheter may decrease the efficacy of cerebrospinal fluid (CSF) drainage or cause an overt system dysfunction. Increasing the risk of recurrent hydrocephalus and increased risks, costs, and time spent in imaging studies and corrective surgical procedures (Gilbert et al., 2009; Huyette et al., 2008). **Figure 1** (Neurosurgical

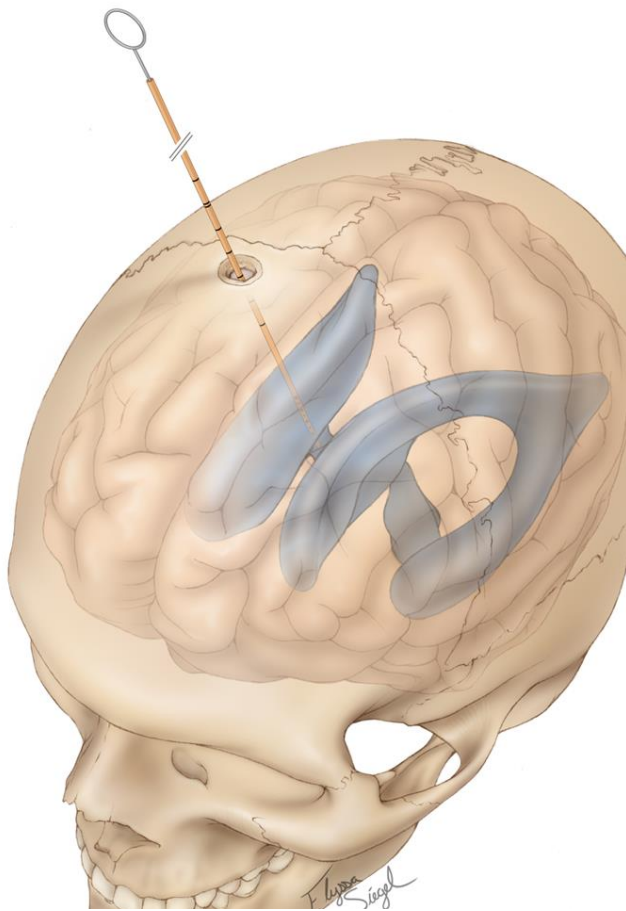


Figure 1. Graphic representation of a ventricular puncture performed through the Kocher point and whose catheter crosses the cerebral parenchyma, the ventricular system and the tip reaches the foramen of Monro. Source: Neurosurgical Atlas, 2023.

Atlas, 2023) shows a visual representation of a correct ventriculostomy whose catheter is ideally positioned.

Some factors that may influence an accurate catheter placement include the ventricular anatomy, technical aspects, and features related to the patient or the surgeon. In particular,

increased ventricular size and a lower distance to the interventricular foramen are associated with a lower chance of system dysfunction (Ericsson, 2004; Subramonian & Muir, 2004). On the other hand, the ventricular puncture's accuracy and the procedure's success also depend on the surgeon's expertise (Yudkowsky et al., 2013).

Surgical skills demand high precision and must be maintained through continuous and repetitive training and feedback (Belykh & Byvaltsev, 2014; Choque-Velasquez et al., 2018; Ericsson, 2004).

Access to virtual simulators is an effective tool for systematic practice (Persky & Lewis, 2019), and they have been studied in different interventions (Alaraj et al., 2015; AlZhrani et al., 2015; Delorme et al., 2012; Gmeiner et al., 2018; Schirmer et al., 2013; Teodoro-Vite et al., 2021). The main advantages of using these systems include the possibility of exhaustive training in a controlled environment and less risk for the patients. Besides allows the incorporation of metrics to objectively assess the trainees' performance and provide valuable feedback (Muralidharan, 2015). Augmented reality (AR) has also been increasingly studied in surgery. It provides visual assistance in the location of anatomical targets in preoperative planning and as intraoperative guidance (Ayoub & Pulijala, 2019; Cabrilo et al., 2014; Cutolo et al., 2017; De Paolis et al., 2022; De Paolis & De Luca, 2019; De Paolis & Ricciardi, 2018; Eagleson & Ribaupierre, 2018; Jud et al., 2020; Kersten-Oertel et al., 2015). AR has been successfully used to increase the success rate of ventricular puncture procedures (Hooten et al., 2014; Schneider et al., 2021; Yudkowsky et al., 2013). However, costs remain a significant limitation for implementing this technology.

In the ventriculostomy procedure, the need to improve puncture quality has been found due to two main factors:

- a) The rate of misplaced catheters is as high as 20%, and one study (Toma et al., 2009) raises the need for practice change. This is because the prognoses are not favorable and there is a high risk when reoperating on a patient who is already in a delicate state.

- b) During the operation, the neurosurgeon takes into account “virtual” references to perform a ventriculostomy, as well as characteristic anatomical points of the patient. However, it is not enough since factors such as ventricular size, intracranial displacements, or deformations influence the selection of the initial reference point for puncture.

This exercise consists of releasing intracranial pressure, derived from inflammation of the cerebral ventricles, through which cerebrospinal fluid circulates.

The procedure consists of inserting a ventricular drainage catheter and positioning its tip over the foramen of Monro (or interventricular foramen) (Gray et al., 2021). Previously, it was necessary to make an incision on the skin, the skull, and the dura mater, which must be accessed through the Kocher point (García Navarro & Castillo Velázquez, 2016). The ideal puncture is parallel to this point and Monro's foramen. Through this reference, it is through which, in a straight line and without pivoting, the catheter must cross the brain parenchyma, the ventricular wall (ependyma), and finally reach the interventricular foramen. The main problem in the operation lies in calculating the location of the aforementioned foramen, a task that is not trivial and therefore is considered by specialists as a "blind" procedure. The methodology for locating this point consists of previously taking two anatomical reference points, located below the auditory tragus and the internal ocular canthus relative to the puncture hemisphere. An imaginary layout of these landmarks is made, and they intersect with the puncture trajectory, which converges on Monro's foramen.

2.1. RELATED WORK

In this section, a brief and comparative review is made of the works found in the state of the art, related to ventriculostomies and their applications with augmented reality, and the metrics used to measure performance and precision in the punctures performed by the participants of these studies.

2.1.1. VentroAR

(Bagher Zadeh Ansari et al., 2022) developed an augmented reality-based application for ventriculostomy punctures through Keen's point. An optical tracking device was used to obtain the position and orientation of the patient's skull, the tool, and the HoloLens. In the study, a hologram is manually recorded on the physical model through the "tap air gesture" feature. The accuracy of the registration was compared through the root mean square error of a registration based on landmarks printed on the skull model and with the help of the tip of the tool. In said study, a mean square error of 8.27 ± 4.0 mm in registration accuracy and a mean square error of 10.64 ± 5.0 mm in targeting accuracy were reported. In addition, the distance error was calculated for each dimension in the planes, where the z-axis presented a greater error (11.67 ± 9.34 mm) and that is attributed to the limitation of HoloLens to provide an effective perception of depth. The study analyzed the distance between the puncture point and the projected point on the trajectory line or radial error (RE) and the distance between the projected point and the target point or depth error (DE), as well as a scale survey System Usability Index (SUS) and the NASA Task Load Index (NASA TLX) for assessing cognitive load and effort in using the system. The author concludes that the system is acceptable for training and planning purposes but not accurate enough for neurosurgical practice.

2.1.2. Augmented reality-assisted ventriculostomy

In the work reported by (Schneider et al., 2021), emphasis is placed on the development of an augmented reality tool to provide the neurosurgeon with guidance during a ventriculostomy, to improve the accuracy and safety of the procedure. Microsoft HoloLens headsets were used for holographic projection of the patient model onto a 3D-printed physical model. The Vuforia framework was used to register the two models employing QR markers located on the physical model. In this configuration, the author includes 5 interchangeable ventricular systems adaptable to the patient's anatomy.

One hundred different patient scans were used for automated training and segmentation to create a 3D model of skin, bone, and lateral ventricles. The algorithm was later used to create the holograms displayed in the tests.

Five challenging ventricular cases whose morphology varied in size and abnormalities were selected. One of the notable features of the 3D printed model is the convexity of the skull referring to the "skull cap" which can be fixed and exchanged after a craniotomy. With the help of a video game controller, the user can enable and disable anatomical elements such as the skin, skull, ventricular system, Kocher's point, and puncture trajectory.

Eleven participants (6 neurosurgeons and 5 neurosurgery residents) took part in the study. Each participant performed two trephinations and placed a total of 10 EVDs in 5 skulls. A successful ventriculostomy ("hit") was considered as an offset between the reference point of the frontal horn and the tip of the catheter. If an attempt was unsuccessful ("miss"), the deviation of the puncture in progress to the reference trajectory is calculated by calculating the vector from the Kocher point to the target reference point, then the EVD vector. The error is considered as the distance between the final insertion point of the EVD and the target point.

A digital caliper was used to determine the registration error, resulting in a mean error of the three axes (XYZ) was 3.06 ± 2.47 mm. On the other hand, the mean error in a successful puncture as the measured distance between the EVD and the reference point was 5.2 ± 2.6 mm. The standard deviation from the target point in millimeters was 10.9 ± 4.1 mm.

On the other hand, three of the participants performed a second round of punctures, where a mean error in successful punctures of 4.3 ± 1.7 mm and a mean error in failed punctures concerning the target of 3.9 ± 2.0 mm were recorded. Based on the above facts, the author observes a significant improvement in the success rate and precision of punctures.

2.1.3. HoloQuickNav

In the document reported by (Baum et al., 2019), an HMD-based navigator is created with HoloLens and Unity3D and whose model registration can be seen manually and with a remote control. This study compares metrics related to the location of an entry point in a patient's skull.

The author reports a registration $< 5\text{mm}$ 65% of the time during the intervention of an expert, while during the participation of novices, the registration was within the acceptable range 94% of the time.

Four metrics were obtained which concern 1) Drill-tip distance: the Euclidean distance between the entry point defined by a commercial navigator and that of the user. 2) Distance to lesion: the closest distance between the user's trajectory and a point (center of a lesion). 3) Drill angle error: the angular error in the trajectory of the participant relative to the golden standard (entry point defined by a commercial navigator). 4) Angle to lesion: the angular error assuming that the tip of the participant's tool is optimal, relative to the center of the lesion given the golden standard.

The results obtained concluded that augmented reality through HMD improves surgical planning and target location in clinical and simulated settings.

In this document, we propose an AR simulation model for ventricular puncture training aimed at improving the accuracy of the procedure and introduce novel metrics for its assessment.

The goal of this study is to provide metrics that evaluate the quality of punctures in ventriculostomies. A search in the state of the art has found that distance errors between a point defined by the system and that of the puncture generated by the user are generally evaluated. The addition of objective metrics that allow us to observe beyond whether the catheter is inside the ventricles may also help the neurosurgeon prevent errors in the punctures performed in the operating room. This work also allows evaluation of which region of the ventricular system the puncture was performed. This is important because if a

puncture is contralateral to the puncture side, it represents a risk for the patient, even if the catheter is outside the cisterns or has passed through them.

Currently, a similar study has been found in terms of metrics regarding the quality of ventricular punctures, but said system is oriented towards interaction through virtual reality (Schirmer et al., 2013), so this motivates us to explore whether the proposed measurements influence an environment based on augmented reality and of course, how to improve them in future work.

In addition, in the works in which reference is made, a deficiency has been found regarding the registration of virtual models with physical ones. It is very common to find HMD-based systems, and more specifically under the use of Microsoft HoloLens I, where registration and field of view problems have been found.

Emphasis is also placed on the registration of virtual models with the physical ones and on improving the error in precision in this section. We are motivated to integrate this system not only as an educational model in a simulation classroom but also as a preoperative planning tool and especially as an intraoperative tool. It is for this reason that we must submit the neuronavigator to a validation process and therefore reduce the registration error to the maximum.

CHAPTER 3

INTEGRATION OF A PATIENT MODEL TO AN AUGMENTED REALITY NAVIGATION SYSTEM

3.1. THE PATIENT MODEL

A set of CT images of a patient diagnosed with hydrocephalus syndrome was selected as a clinical case. CT images were segmented using 3D Slicer software (Fedorov et al., 2012) to obtain reconstructed anatomical models of the skull, skin, and cerebral ventricles.

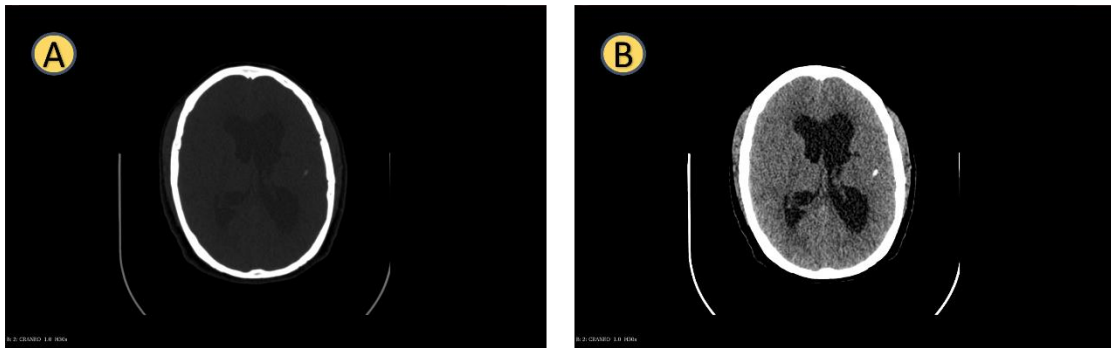


Figure 2. A) Computed tomography image without enhancement in the image. B) the image of the case of tomography after image enhancement. The cerebral ventricular system is more clearly visualized.

The software allows the use of segmentation algorithms on the 2D images, then the 3D reconstruction is performed at the time of visualization.

When loading the CT file, an enhancement is made in the intensity of the image to visualize anatomical structures that delimit the bone with the brain parenchyma and the ventricular structures of the clinical case. **Figure 2** shows the clinical case in 2D top view with and without enhancement of the series of images.

The software generates groups of segments where we can establish the area and volume of interest and each segment can be identified by a name, for example, "brain" or "cerebral ventricles", as well as by colors, which makes it possible to better distinguish the selection.

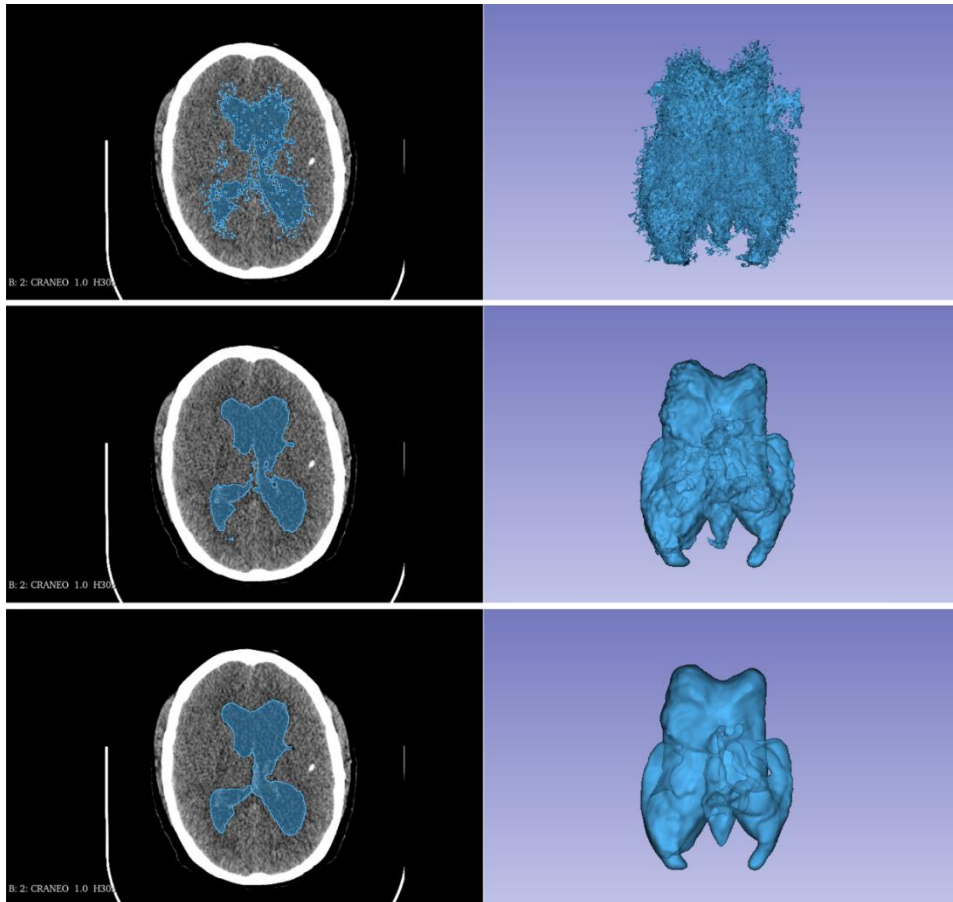


Figure 3. Segmentation process of the ventricular system in 3D Slicer. Top: preliminary segmentation of the cerebral ventricles using simple thresholding. Middle: median filter application to segmentation by thresholding. Below: application of a Gaussian filter to smooth the anatomy.

As shown in **Figure 3**, a segment is assigned a set of editing functions and segmentation algorithms. In the case of our tomography, we made use of the thresholding technique considering a minimum and maximum range of intensity values in the image. It was enough to apply a simple segmentation to the skull. In the case of ventricular anatomy, an additional process was required to which the median filter with a kernel size of $7 \times 7 \times 3$ pixels was applied. Subsequently, the structure was smoothed with a Gaussian filter with a standard deviation of 1.5 mm.

A refinement of the anatomy was manually made in the software Blender (Hess, 2010), mainly the correction of non-manifold elements and decimation to reduce the mesh size but maintain the topology.

Afterward, a physical model of the patient's skull was printed using additive manufacturing with commercial 3D printing equipment, the Original Prusa™ i3 MK3S 3D printer. The models were printed using PLA material plus PVA as support material. A high detail setting with a layer resolution of 0.15mm and a 20% infill density was used to maintain the minimum hardness required for the simulation. Then with the printed model, the burr hole was made with a craniotome at Kocher's point, located by completing the following measurements: 10cm from the nasion following the midline, then 3cm lateral to the midline and confirming that it is 1-2 cm anterior to the coronal suture, this being the ideal point for catheter insertion (Mostofi & Khouzani, 2016), corresponding to the intersection of the lines that join the projection of the external auditory canal with the ipsilateral internal canthus.

Then, with the patient's model placed in the simulator in a dorsal decubitus position, with the head slightly flexed with 0 degrees of rotation (Mostofi & Khouzani, 2016),

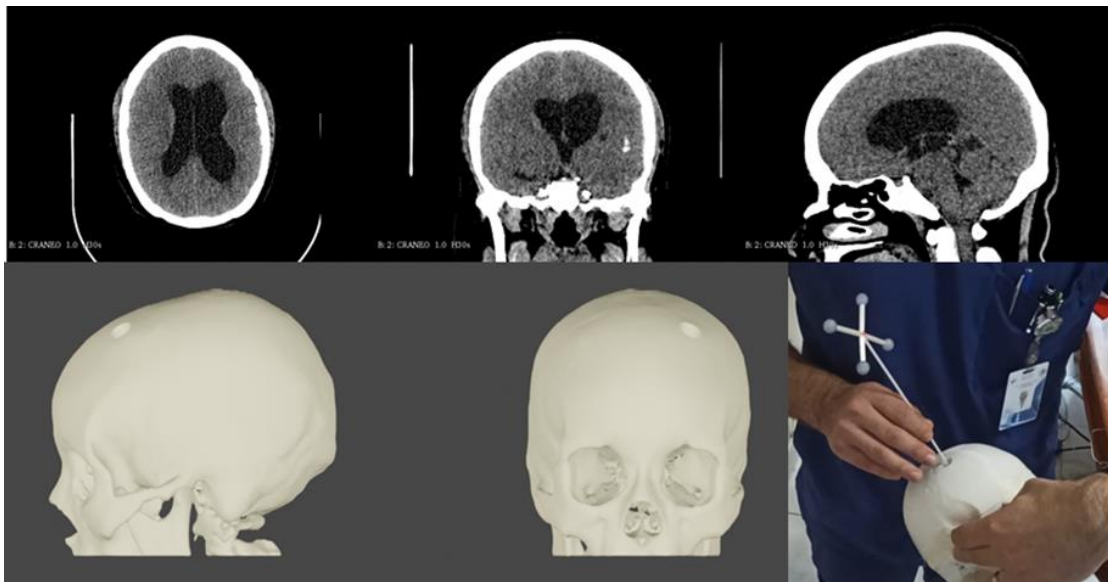


Figure 4. Selected clinical case from a patient diagnosed with hydrocephalus disorder. From the CT image study to the 3D reconstruction of the virtual model, and the 3D printing of the physical model.

the spatial location of the Kocher point was recorded. This was done with the help of the optical tracker and by palpating the edges of the burr hole with the stylet and identifying their central point. From the registration of the Kocher point, the ideal insertion guides were established in the virtual model, and the target point in Monro's foramen in the virtual model by following the ideal line, in this case, 5cm from the Kocher point.

Figure 4 illustrates the result of the reconstruction of the clinical case.

3.2. THE AUGMENTED REALITY SIMULATOR

The AR simulator consists of an arm with two passive links with 2 degrees of freedom which support the skull and which, in turn, allows the object to be repositioned: one translational and the second rotational, which allows changing the position and inclination of the printed skull, respectively. The system contains a commercial optical tracking module (Optitrack V120: Duo, Optitrack) for skull location, a stereo camera (Zed Mini, Stereolabs), and a 3D-printed puncture tool.

The system (**Figure 5**) also contains a computer workstation module that hosts the augmented reality software.

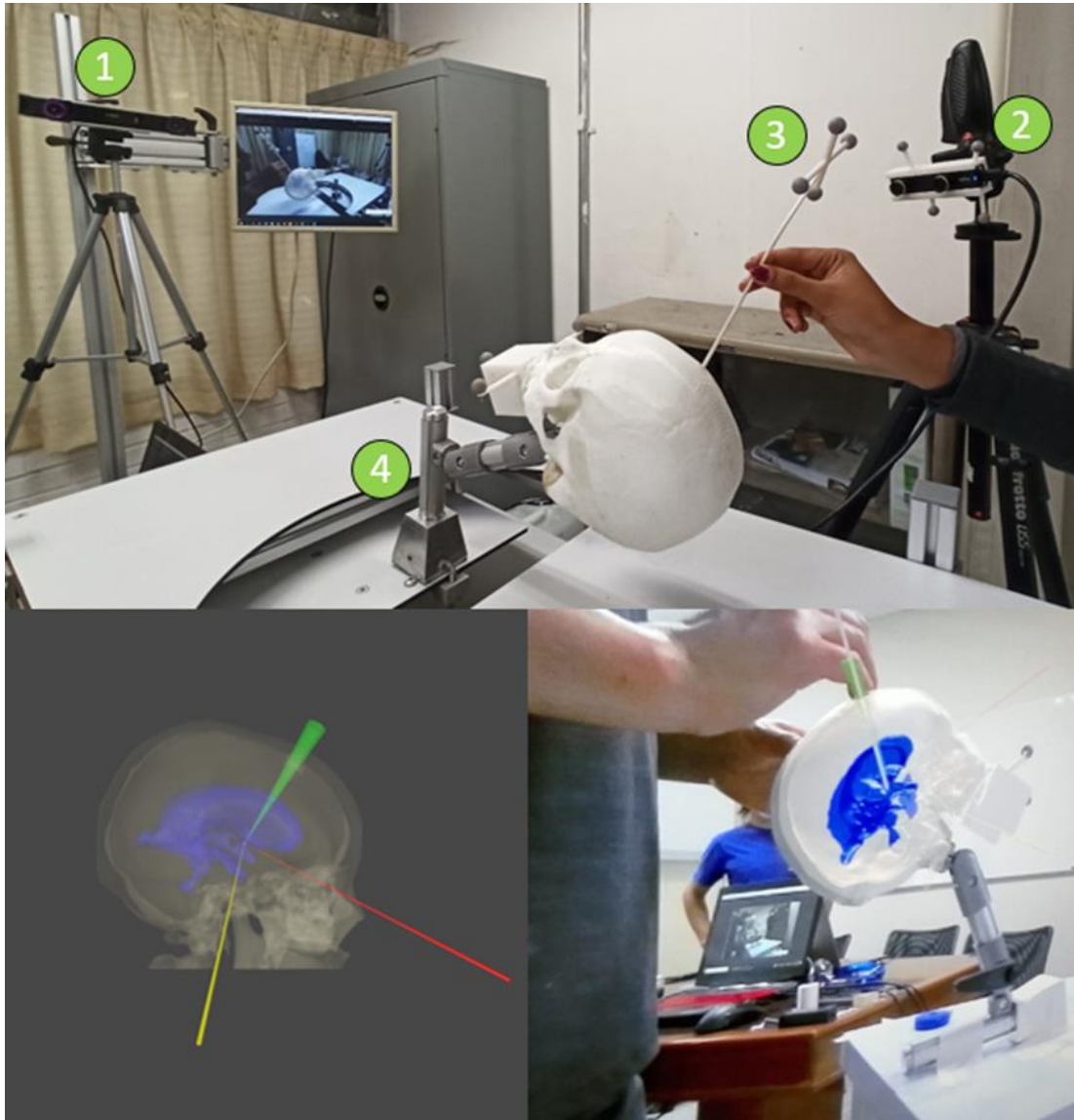


Figure 5. The complete setup of the augmented reality simulator of ventriculostomy procedures. In top: 1) is the optical tracker for monitoring in real-time the pose of the elements in the scene; 2) the RGB stereovision camera for the acquisition of the video frames of the real scene of the physical printed model; 3) a rigid replica of the catheter, with a cross-shape marker frame for tracking its position in space; 4) the physical printed model of the patient, with a cubic marker frame for tracking its posture in real-time. Bottom: The graphical 3D model of the anatomies, with the Kocher and Monro reference points, the reference axis crossing (in yellow and red) at the target Monro foramen, and of the ideal trajectories (in green). A sagittal augmented view displayed to the practitioner.

In addition, CAD (computer-assisted design) models of the rigid frame for mounting the patient model, housing the stereo camera, and the puncture tool were modeled, and 3D printed. This was done so that each has a unique localization frame due to its

unique sphere configuration attachments. The optical tracking module locates in real-time all the objects in the scene.

Figure 6 shows a diagram of the navigator information flow for the generation of the augmented reality scene. The physical scene consists of positioning the three objects within the area of vision of the tracker so that the skull, mounted on the arm, the stereo camera capturing the scene, and the catheter always remain visible to the tracker.

The augmented reality scene was developed in Unity 3D (*Unity*®, 2023), which graphically renders a projection in transparency over the physical model, the virtual anatomical structures of bone, and ventricles. Besides Kocher's point, the target (foramen of Monro), and the ideal guiding lines in colors.

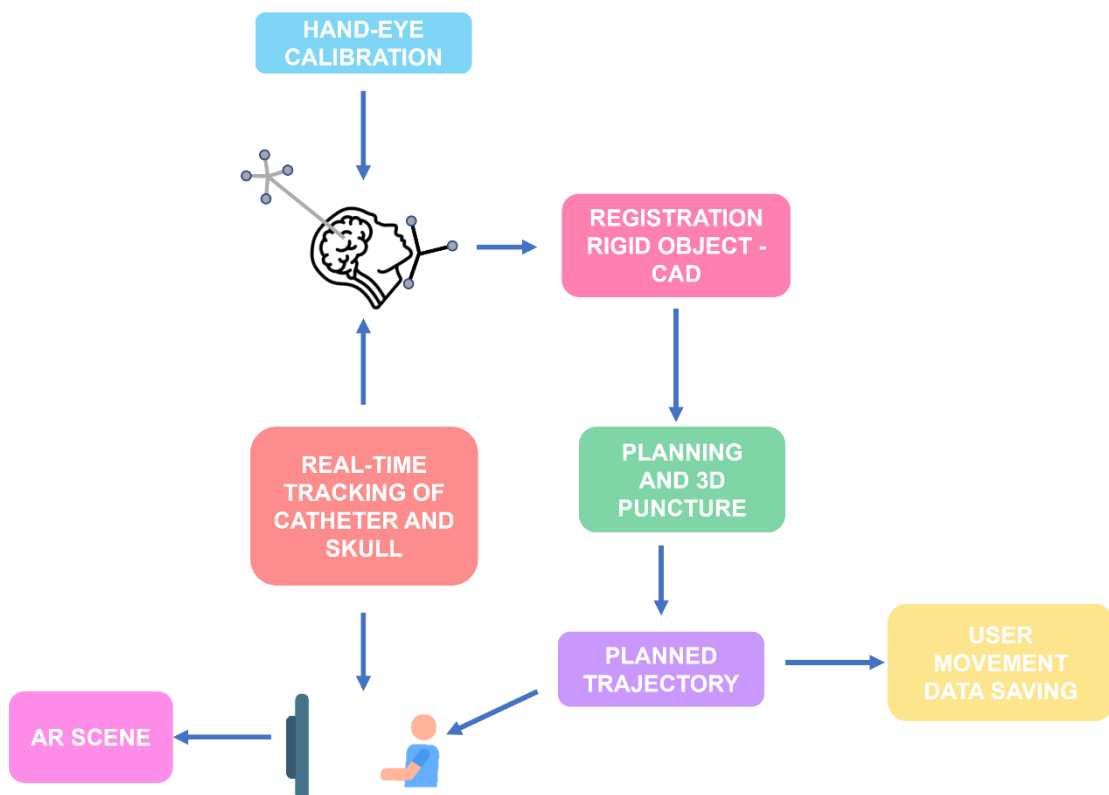


Figure 6. Navigator data flow for the generation of the augmented reality scene for ventriculostomy.

The transparent projection was presented in the sagittal plane and displayed on a flat screen with a frontal perspective concerning the participant's point of view. The final

visual scene allows the participants to perceive the insertion of the physical catheter into the physical model under the guidance of the projected visually augmented information, facilitating the localization of the target point and the correct spatial trajectory of the catheter tip during the punctures. **Figure 7** shows the user interface, which allows evaluating different conditions as required to obtain data for evaluation in improving the quality of punctures.

During the insertion, the software records the position of the catheter tip, besides the poses of the elements in the scene. With this information, the software computes some metrics to analyze the trajectories and accuracy of participants, as detailed in the next section.

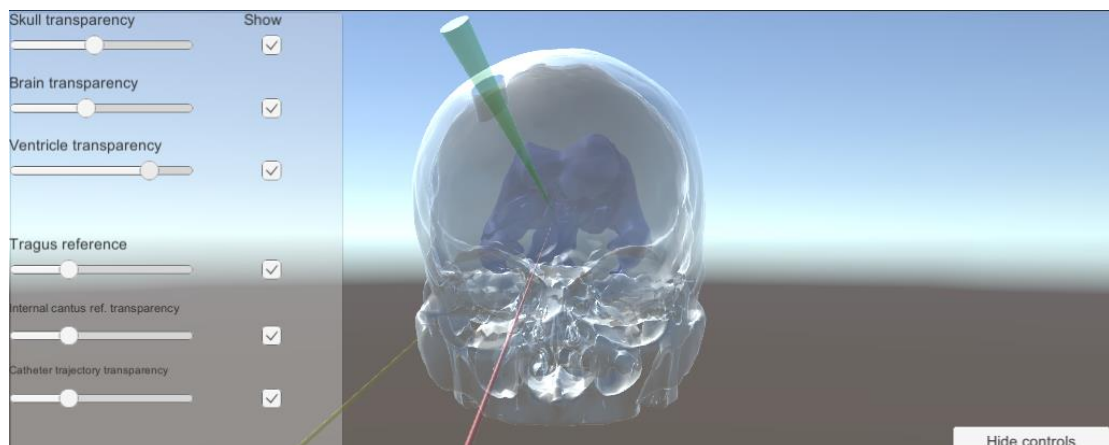


Figure 7. Navigator's user interface. This allows you to vary the transparency and activation state of the interactive elements during the simulation.

CHAPTER 4

ACCURACY MEASUREMENT AND TESTING

One of the most important and challenging steps in the development of the project was to align the projection of the virtual models with the model of the physical scene. During testing, the user should ideally view the anatomical components of the patient on top of the 3D-printed skull, otherwise, this could lead to poor visual feedback to the neurosurgeon and consequently bias the captured data. To achieve a good alignment and a level of reliability compared to the works in the state of the art, the following calibration and measurement tasks were carried out:

- RGB camera calibration.
- Hand-eye calibration (AXXB).
- System error measurement.

4.1. Camera calibration

Camera calibration has always been the most important component in the design of computer vision applications. The purpose of calibration is to convert the coordinates of a 3D object into coordinates of a 2D image. During image capture through a camera, light from a scene that falls on an object is also captured. Each pixel in the image is associated with incoming light, and errors resulting from misaligned lenses can result in very complex distortions in the final image. The projection matrix is composed of intrinsic and extrinsic parameters and there are some methods to extract

them. The simplest and most used method is the perspective projection method (Fetić et al., 2012).

Distortion caused by the camera lens can be perceived from a raw image. If this is not calibrated and depending on the lens, deformation may be perceived in the periphery of the output image.

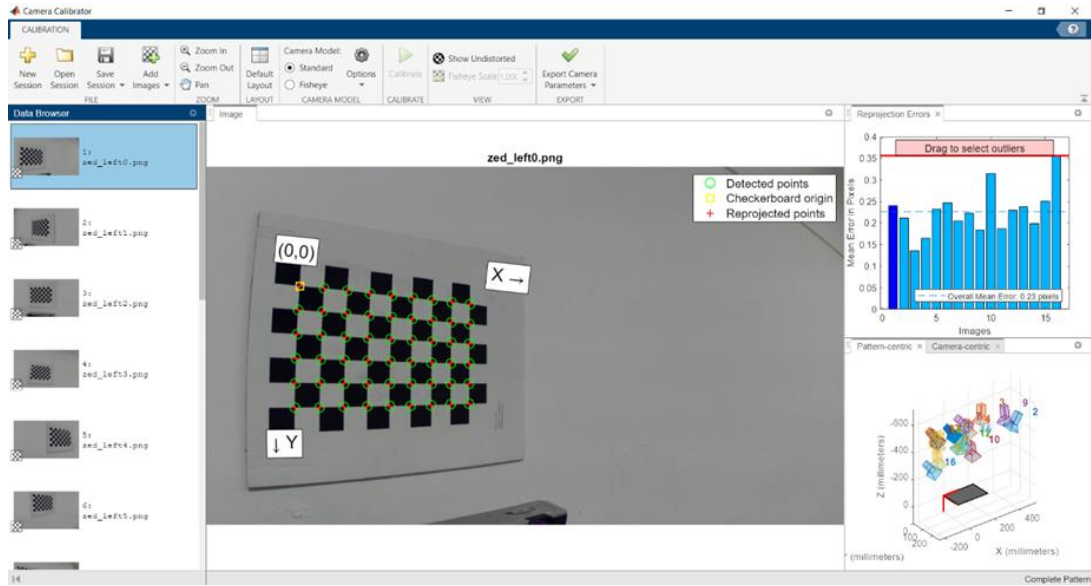


Figure 8. View of the interface of the MATLAB Camera Calibrator tool, whose function allows determining the intrinsic parameters, necessary to undistort the video stream where the virtual models are projected on the scene. Radial distortion is displayed in the calibration pattern.

To undistort the camera image that will project the virtual models, it is necessary to determine the intrinsic parameters, we must determine the matrix A , whose components correspond to the coordinates of the principal point (u_0 , v_0), the focal length (α , β) and the skew of the axes of the image (γ) (Zhang, 2000). This matrix is embedded in the camera object in the scene such that the output image from the camera in the navigator is projected without distortion, where the components of the matrix are given by

$$A = \begin{bmatrix} \alpha & \gamma & u_0 \\ 0 & \beta & v_0 \\ 0 & 0 & 1 \end{bmatrix}$$

(1)

16 images were obtained from the Zed camera of a chessboard for calibration and the MATLAB CameraCalibrator tool was used to determine the necessary parameters to undistort the image stream generated by the camera. **Figure 8** shows the use of the tool with reference images for calibration in detail. The extrinsic parameters are calculated in the same process of camera calibration. The CameraCalibrator tool calculates the position and orientation of the camera to the origin of the chessboard for each take taken.

Although only the left camera is used, it is necessary to consider the intrinsic parameters of both. The parameters of both cameras are necessarily required in the camera object in the navigator software. This receives an OpenCV calibration file using the YAML format.

Two intrinsic parameter matrices A_r and A_l were obtained, belonging to the right and left cameras. The values were applied to the YAML file, where the video stream is undistorted in real-time. The resolution used during the camera calibration was 1280x720px for each of the cameras.

The intrinsic parameter of matrix A_r :

Focal length	(686.9781, 685.8954)
Principal point	(639.9776, 365.0178)
Radial distortion	(-0.1658, 0.0089)

The intrinsic parameter of matrix A_l :

Focal length	(688.3107, 689.0076)
Principal point	(634.9924, 350.0038)
Radial distortion	(-0.1755, 0.0238)

4.2. Hand-eye calibration (AXXB)

To ensure that the projection of the virtual models was correctly aligned with the elements of the real scene, the Hand-eye calibration process had to be carried out.

One of the factors that cause anatomical models to be misaligned is the offset between the camera housing and the camera. In the rigid object configuration that we developed, the camera is inside its casing, and of both, we can only know the position of the casing, since they are tracked thanks to the spheres that it contains. On the other hand, the pose of the camera is unknown. To find the transformation matrix that

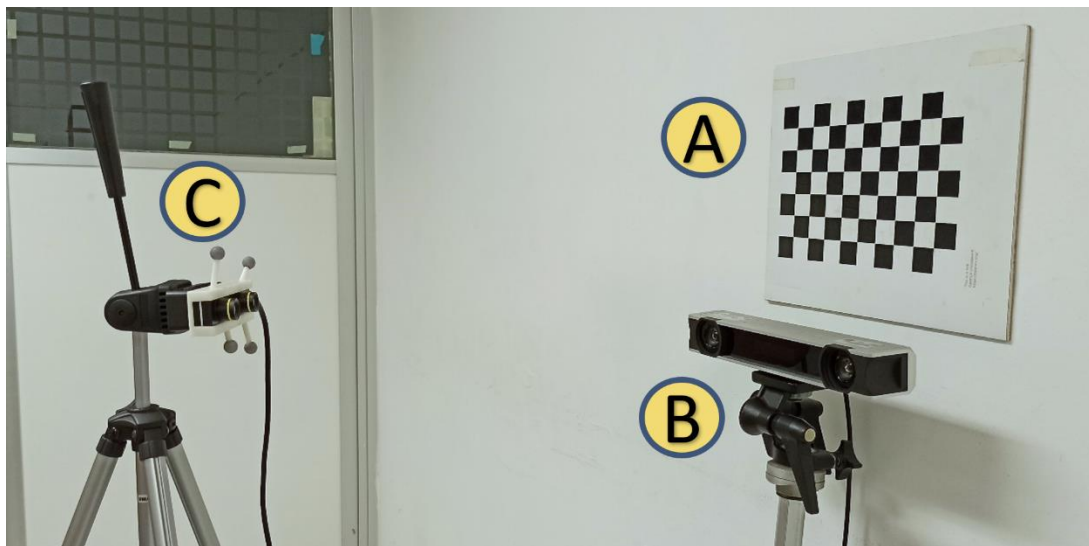


Figure 9. Obtaining camera poses with respect to the chessboard (A) through the extrinsics calibration parameters. Obtaining the physical poses of the camera housing through the optical tracker (B). The camera and its casing (C) change position with each take.

describes the offset between both objects, the positions of both objects must be known.

The aforementioned can be solved by building a double calibration configuration such that to calculate the camera and housing poses the optical tracker and a chessboard calibration pattern are necessary. **Figure 9** shows the necessary composition for the Hand-eye calibration.

When it is required to estimate the position of a camera mounted on a robotic arm where both objects have their three-dimensional space defined (Horaud & Dornaika,

1995; Lai et al., 2018), the Hand-eye calibration method is used. In the developed configuration, the camera housing can be interpreted as the robotic arm.

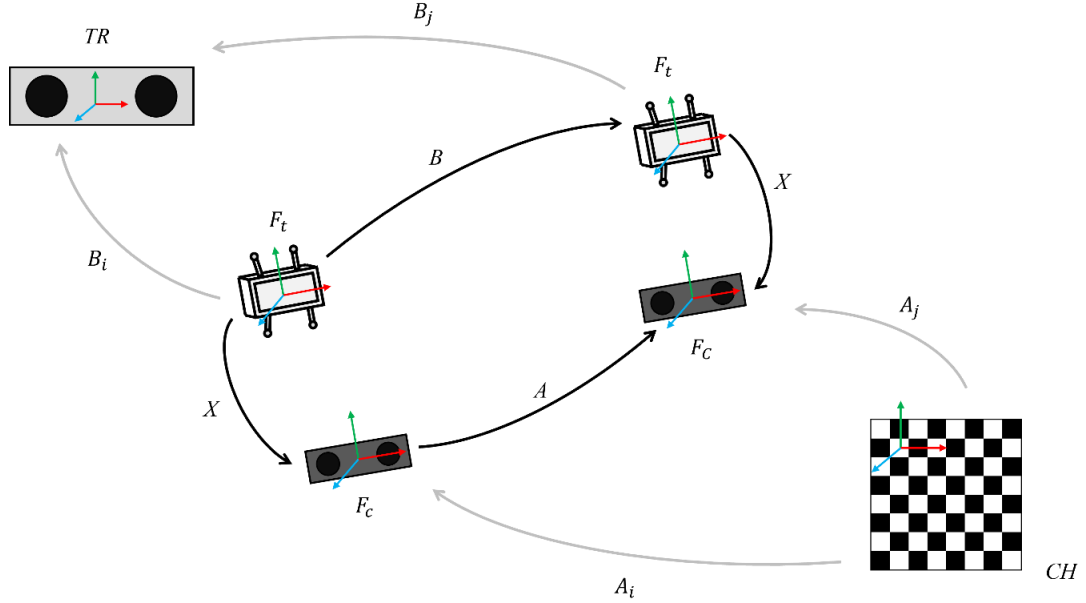


Figure 10. The hand-eye problem, where TR represents the optical sensor frame, F_t represents the case frame, F_c represents the camera frame, and CH represents the chessboard frame.

The hand-eye calibration can be formulated with homogeneous transformation matrices in the form

$$AX = XB, \tag{2}$$

where $A = A_j A_i^{-1}$ and $B = B_j^{-1} B_i$.

Where X is the transformation from hand to eye (camera case). A is the motion of the reference frame of the camera. B is the motion of the reference frame of the case. A_i represents the transformation matrix from the world to the camera coordinate system, and B_i represents the transformation matrix from the case to the optical tracker at the i -th pose (**Figure 10**). The transformation A_i is obtained using the Camera Calibrator tool through the extrinsic parameters, and B_i is given by the optical tracking system. To solve the homogeneous equation we need at least two motions with different rotation axis (Wei et al., 2015).

Ten takes of poses from the calibration chessboard and the optical tracker were taken, varying the positions of the camera mounted on its casing. Subsequently, the calculation of the matrix X was made to solve the equation $AX = XB$ using an implementation presented by (Park & Martin, 1994). The solution returns a matrix of size 4x4 where the internal 3x3 matrix represents the rotation and the first three values of the last column represent the translation vector. It must be considered that to enter the rotation matrix, it was necessary to convert that matrix to quaternions.

4.3. Singular Value Decomposition (SVD)

Another problem to solve is to virtually align the models of the skull, the catheter, and the camera with their counterparts from the optical tracker. More specifically, the optical tracker sends to Unity the poses of the physical objects through identifiers, as well as the local positions of the retroreflective spheres of each one. The definition of each of the rigid objects is done offline through the utility software of the optical tracker.

Manually performing this alignment is not easy and a minimal error in the alignment is visually reflected in the execution. To solve this problem, it was necessary to generate new coordinate systems for each of the rigid objects and align these coordinate systems with the virtual ones (CAD models). It is necessary to ensure perpendicularity between the two models.

To solve this problem, a least squares alignment method (Arun et al., 1987) was used that considers two point clouds in 3D space, which are given by the retroreflective spheres sent to the software and the CAD object. Each of the points is expressed in matrices of size 3x1. The relationship of two points in a 3D space is given by the following equation:

$$p'_i = Rp_i + T + N_i,$$

(3)

where, p_i are the positions of the points of a rigid object registered by the optical system, while p'_i corresponds to the set of misaligned points of the CAD model. R is a rotation matrix of size 3×3 , T is a translation vector of size 3×1 , and N_i is a noise vector. In the implementation of this alignment model, the noise is generated by the optical tracker and therefore it is discarded from the equation.

Restating the above equation, we are left with:

$$p'_i = Rp_i + T \tag{4}$$

and therefore:

$$T = p'_i - Rp_i, \tag{5}$$

which translates into finding a rotation matrix R such that it minimizes the sum of the squared differences of the distances between a point and its centroid of a cloud of points $\{p'_i\}$ and $\{p_i\}$ multiplied by the matrix R . If we find R , we can calculate T .

SVD receives as a parameter a matrix H which is composed of the sum of the vector product generated from the distance between a point and its centroid.

Assuming that each point cloud has the same centroid:

$$p = p' \tag{6}$$

where

$$p \triangleq \frac{1}{N} \sum_{i=1}^N p_i \tag{7}$$

and

$$p' \triangleq \frac{1}{N} \sum_{i=1}^N p_i$$

(8)

The distance between a point and its centroid is given by:

$$q_i \triangleq p_i - p$$

(9)

$$q'_i \triangleq p'_i - p'$$

(10)

So, the matrix H can be built through:

$$H = \sum_{i=1}^N q_i q'_i$$

(11)

Product of the application of SVD through the MathNet library, the factorization $H = U\Lambda V^t$ was obtained, where U is a unitary matrix of size $m \times m$, Λ is a matrix of size $m \times n$ made up of the singular values of H on its main diagonal ordered from largest to smallest, and V is a unitary orthogonal matrix of size $n \times n$. Therefore, the matrix X can be calculated by:

$$X = VU^t$$

(12)

From the above it can be defined:

$$\text{If } \det(x) = +1, \text{ then } R = X$$

(13)

$$\text{If } \det(x) = -1, \text{ the algorithm fails.}$$

(14)

If $\det(x) = -1$, it implies a reflection, so the rotation matrix will be given by

$$X = V'U^t \tag{15}$$

Such that

$$V' = [v_1, v_2, -v_3] \tag{16}$$

Integrated the calculations to find the rotation matrix R , as well as to find the translation vector T in the Unity script resulting in an alignment every time the scene is refreshed.

4.4. System error measurement

It is essential to provide as an additional aspect the measurement of the augmented reality system error. A calibration process consisting of iterative palpating predefined landmarks under the system guidance was carried out, first on a 3D printed calibration frame (**Figure 11**) and then a set of anatomical landmarks over the skull.

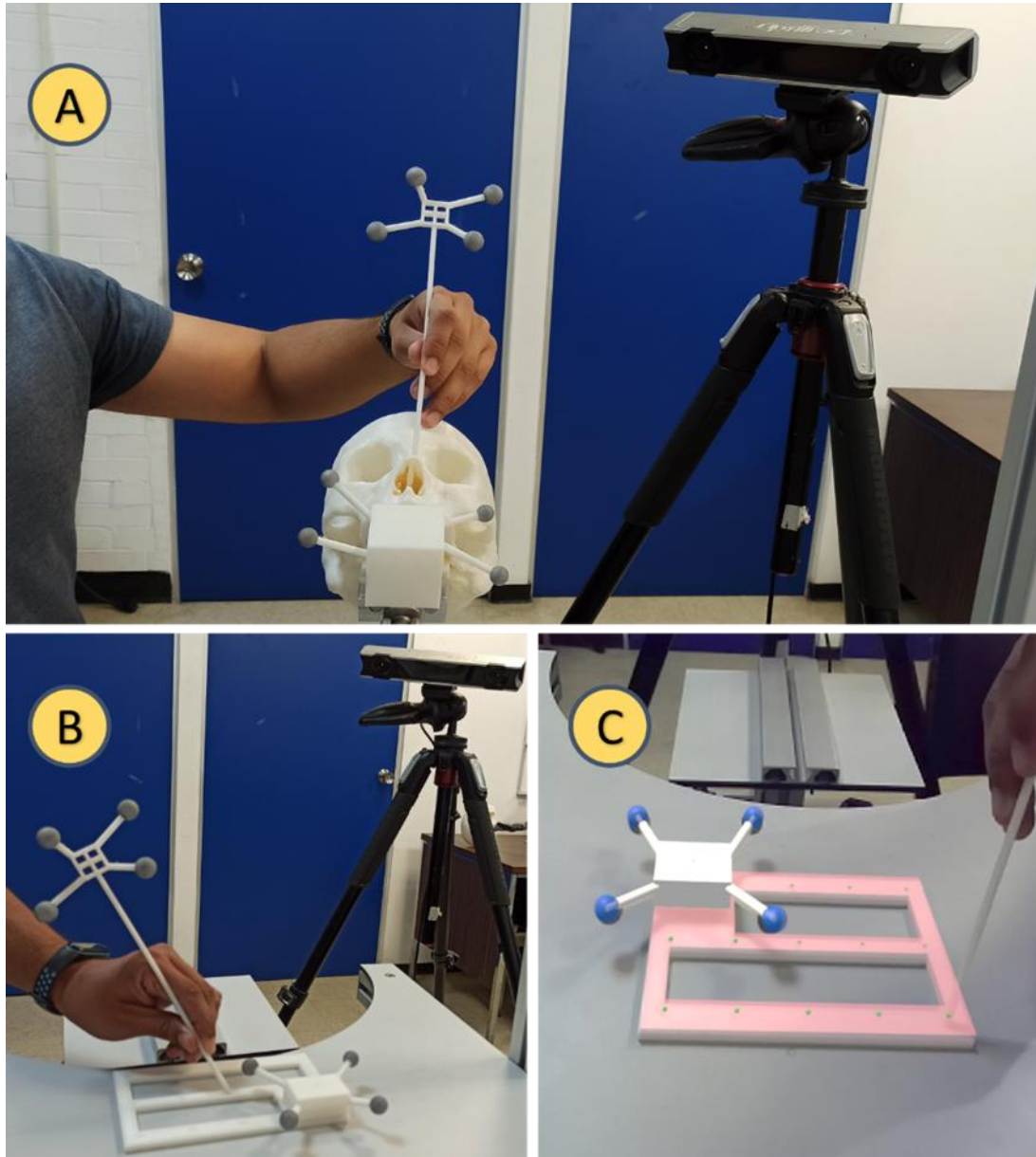


Figure 11. The system error measurement process through an iterative fiducial probing process. The average distance between a set of fiducial points and the tip of the catheter is calculated. A) Palpation of craniometric reference points in the puncture model. B) Palpating of known points with the catheter model in a calibration frame. C) Visualization of the augmented model on the calibration frame.

The navigation system recorded the spatial coordinates of these characteristic points on the 3D models and was compared using an average distance metric concerning those generated by the user with the aid of the catheter and using the augmented projection. The measurement of the error with the calibration frame of 0.86 ± 0.5 mm was obtained, representing the tracking error, while an error of 1.13 ± 0.3 mm with the skull landmarks, representing the location error with the augmented reality system.

CHAPTER 5

AUGMENTED REALITY NAVIGATION FOR VENTRICULAR PUNCTURE: EXPERIMENTS

5.1. THE OBJECTIVE OF THE STUDY

The main objective of the study was to evaluate to what extent the use of augmented reality through the proposed model can be helpful for the training of ventricular neurosurgical procedures. Additionally, to investigate to provide quantitative metrics useful in evaluating the acquired skill during the training under augmented reality visual assistance.

5.2. PARTICIPANTS

Forty-eight participants were invited to the study, including medical students, neurosurgical residents, fellows, and neurosurgeons from the Neurology and Neurosurgery National Institute of Mexico "Manuel Velasco Suárez". Participants were divided into four groups: 5 experts (neurosurgeons), 12 seniors (fellows and residents in years 4-5), 11 juniors (residents in years 1-3), and 18 novices 18 (medical students without any experience in neurosurgery). The study was reviewed by the Institute's ethics committee.

5.3. EXPERIMENTAL PROCEDURE

Participants performed a series of ventricular punctures in the 3D printed model of the patient in three experimental conditions, as follows.

Positioning: The participant was asked to stand in front of the worktable that simulated a surgical table and found the cranial model printed in 3D from the study to

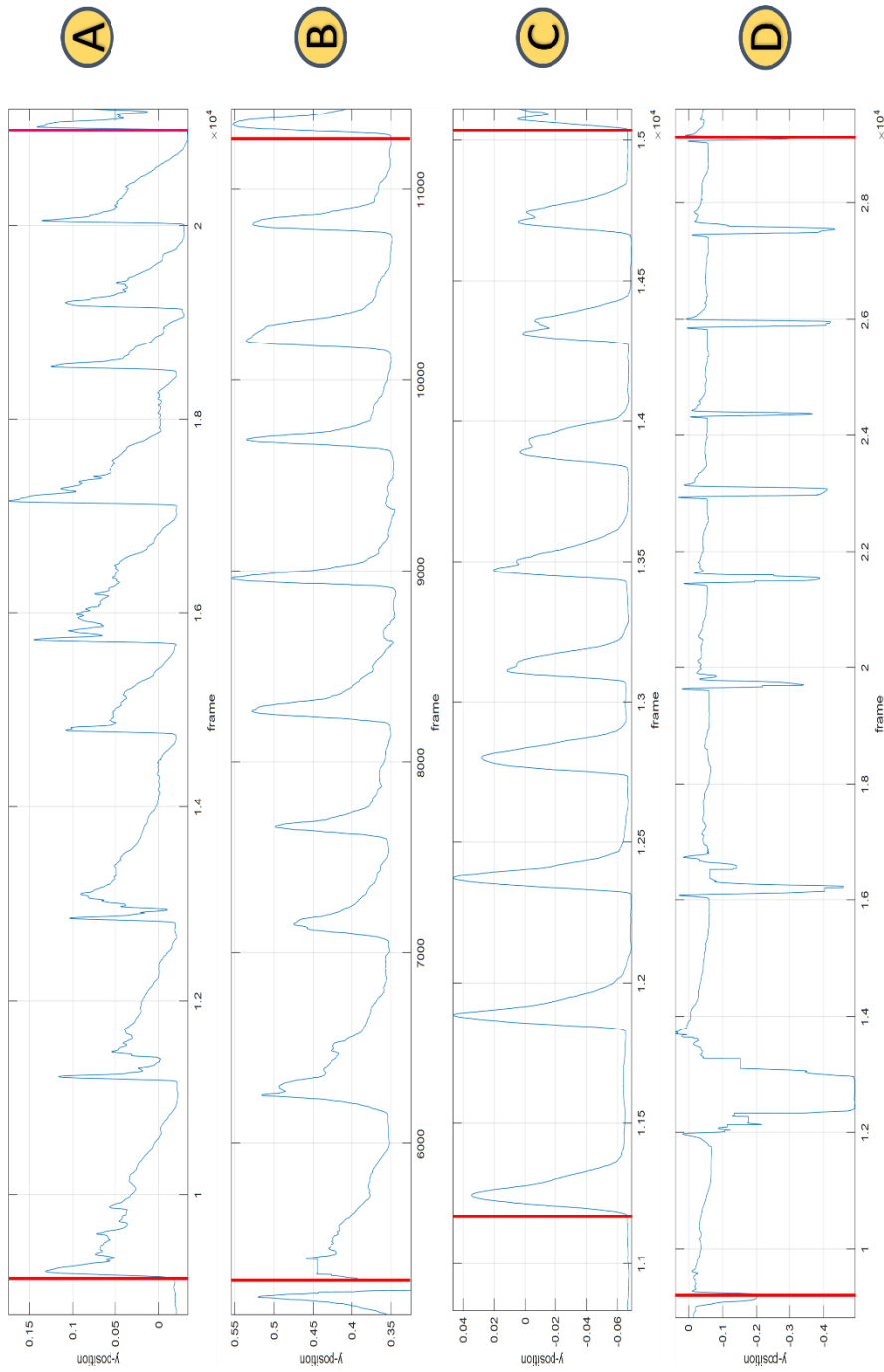


Figure 12. Catheter tip movements captured during a series of punctures in AR-Condition (Red vertical lines). A) Novice punctures. More care and slowness can be observed, as well as punctures in shorter valleys. B) Punctures of Junior. Care is observed in the punctures but a faster descent towards the valleys. C) Punctures of a Senior. Greater speed is observed when descending towards the valleys and with a longer and more stable depth at the base of the valley. D) Punctures by an expert. Fast punctures and retractions and variation in the depth of the valleys can be observed, as well as longer periods before making a decisive puncture.

the hole. Then was asked to locate with his/her hands on the 3D printed cranial model the anatomical structures nasion, and medial canthus ipsilateral to the puncture site. Then took the stylet with the retroreflective spheres and focused on the drill bit.

Initial evaluation puncture (Pre AR condition): The participant made the puncture through the burr hole, introduced the stylet with reflective spheres, and notified the technical team when considered that it was already in the target position (Monro hole). The technical team then recorded the position coordinates of the stylet with respect to the target, the distance to the ideal trajectory, and its angulation. The first puncture for that user was then recorded.

Training punctures (AR condition): After a pause of some seconds, the participant was asked to be positioned again in front of the cranial model and the worktable. Then completed a series of 10 training punctures as before, now receiving visual assistance with the augmented reality scenario, showing in transparency the projection of the ventricles, the target at the Monro foramen, and the guiding guides showing the ideal path.

Final evaluation puncture (Post AR condition): After another pause, the participant performed a second manual puncture without AR visual assistance, like in the initial evaluation puncture.

During all the procedures, the motion path of the tip of the stylet was recorded, and a set of metrics was computed for posterior analysis. **Figure 12** shows four examples of punctures generated by each of the categories evaluated. In them, the intensity of the movements can be visually observed in the most visually representative axis with respect to each captured frame.

5.4. MEASUREMENTS

To compare the practitioners' skills before and after the training, the simulator monitors and records real-time information on the executed punctures. Then, for every executed puncture, some metrics were off-line computed for the subsequent analysis of the participants' performance. Such metrics were proposed to assess two aspects: the accuracy in reaching the target point and the quality of the executed task. As in similar approaches (Schirmer et al., 2013; Schneider et al., 2021), the accuracy was evaluated by computing the spatial errors of the final reached position with the

tip of the catheter to the final target at the Monro foramen. The error metrics include the 1) spatial error in 3D and the errors in the 2) coronal, 3) traversal, and 4) sagittal (the visually augmented) planes. For assessing the improvement of the movements, the metrics include 5) the angle of the estimated line from the starting and ending points of the trajectory computed in the visually augmented plane (angle trajectory). 6) The linear distance from the starting to the ending point of the executed trajectory (ideal path length). 7) The total length of the recorded trajectory of the tip of the catheter, from the starting point outside the burr hole to the final reached position (path length). 8) The ratio between the length of the executed real and ideal trajectories (path ratio), where a ratio close to 1 indicates a linear trajectory. In contrast, values greater than 1 indicate more erratic and curved trajectories. 9) The difference between the ideal and the executed path, computed as the area under the curve resulting from the difference between the real and ideal paths. In other words, the accumulative path error (path difference).

5.5. STATISTICAL ANALYSIS

A series of multivariate analyses of variance (MANOVA) was applied to the observed metrics following two factors experimental design: 3 task conditions (manual Pre-AR puncture, AR-assisted puncture, and manual Post-AR puncture) x 4 groups (experts, seniors, juniors, and novices). For the Pre and Post manual conditions, a set of single metrics was acquired per condition since the participants performed single punctures before and after the training. For the AR-assisted puncture, the analysis included the mean values of the observed metrics of the series of executed punctures during the training. The tests were carried out in SPSS v.20. Descriptive statistics were computed accordingly.

5.6. COMPARISON BETWEEN VENTRICULAR PUNCTURE SYSTEMS

Many works related to navigation and neurosurgery have been reported in the literature, the topics range from exploration, tumor resection, operations on the spine, and its relationship with the spinal cord, which is partly related to neurosurgery. In

this section, a comparison is made only of the main characteristics of the ventricular puncture systems found in the state-of-the-art. The following comparative table (**Table 1**) is not intended to underestimate the work carried out by other institutions, but rather to make a brief list of characteristics between them and the proposal that we make in this writing.

System	Num. participants	Reported Metrics	Num. of integrated clinical cases	Registration error reported	Puncture error reported	Technologies
VentroAR	15	<ul style="list-style-type: none"> • Registration error • Puncture error • Depth error analysis 	4	8.27±4.0 mm	12.5±8.5 mm	<ul style="list-style-type: none"> • HoloLens • Optical Tracker • 3D Printing • Videogame controller
Augmented reality-assisted ventriculostomy	11	<ul style="list-style-type: none"> • Registration error • Puncture error • Successful puncture (inside ventricle) • Missed puncture 	5	3.06±2.47 mm	5.2±2.6 mm, 3.9±2.0 mm	<ul style="list-style-type: none"> • HoloLens • 3D Printing • Videogame controller
HoloQuick Nav	13	<ul style="list-style-type: none"> • Drill angle error • Puncture error 	2	NA	NA	<ul style="list-style-type: none"> • HoloLens • Mannequin • Videogame

		<ul style="list-style-type: none"> • Drill tip distance • Drill location and angle • Distance to lesion 				controller
BACSIM Ventricular	48	<ul style="list-style-type: none"> • Spatial error in 3D • Errors in XYZ planes • Angle trajectory • Linear distance starting-ending points • Total length of recorded trajectory • Ratio of length executed vs. ideal trajectories • Difference executed-ideal paths 	1	1.13±03 mm	22.0±18.5 mm, 5.6±5.0 mm	<ul style="list-style-type: none"> • Optical Tracker • RGB Camera • 3D Printing

		<ul style="list-style-type: none"> • Registrati on error • Precision error • Puncture location with respect to the ventricula r system 				
--	--	---	--	--	--	--

Table 1. Comparison between augmented reality systems for ventricular puncture interventions.

CHAPTER 6 RESULTS

	Experience				p-value
	Student (n=18)	Junior (n=11)	Senior (n=12)	Expert (n=5)	
Path Metrics					
Angle [°]	64.0±2.18	65.78±2.79	66.53±2.68	64.12±3.91	NS
Ideal Path Length [mm]	125.87±7.52	107.37±9.62	124.85±9.21	120.81±13.45	NS
Path Length [mm]	171.56±74.05	176.17±107.27	169.69±92.04	217.18±153.91	NS
Path Ratio	1.37±0.50	1.71±0.54	1.39±0.44	1.76±0.79	0.00087 (F=5.868)
Path Difference [mm ²]	5.65±5.03	6.47±5.34	6.88±8.03	9.88±9.07	NS
Target Error					
Coronal Plane (XY) [mm]	6.12±5.43	6.25±6.98	4.70±2.47	11.68±22.75	0.082 (F=2.282)
Traversal Plane (XZ) [mm]	11.71±16.64	4.87±6.29	7.87±9.91	10.58±11.41	0.005 (F=4.461)
Sagittal Plane (YZ) [mm]	11.41±12.84	6.40±6.27	7.96±6.66	10.36±12.95	0.031 (F=3.014)
Spatial [mm]	12.53±15.90	7.47±7.61	8.70±7.58	14.74±22.73	0.052 (F=2.648)

Table 2. Observed metrics of the ventricular puncture comparing the execution of the procedure by experience level.

The series of MANOVA applied over the executed trajectories during the ventricular punctures reveals the main factor effects of both experience level (**Table 2**) and task condition (**Table 3**) over some of the observed metrics. A main factor effect of experience was revealed over path ratio ($F(3,139)=5.868$, $p=0.00087$), with students and seniors with lower values than juniors and experts, as confirmed by the Bonferroni posthoc test. No main factor effect of experience was revealed on angle, ideal path length, path length, and path difference. Regarding the accuracy of the puncture, the main factor effect of

experience was revealed in the spatial error ($F(3,139)=3.821$, $p=0.012$), the errors in the coronal, sagittal (the visually augmented plane), and traversal planes, in general with lower errors for juniors and seniors compared to students and experts, according to the corresponding Bonferroni posthoc tests.

Regarding the effect of task condition, the MANOVA reveals the main factor effect over all the metrics, except angle, followed by interesting differences confirmed by the subsequent post hoc tests. For the ideal path length ($F(2,139)=3.92$, $p=0.022$), with smaller lengths before the training (Pre AR). For the path length ($F(2,139)=5.753$, $p=0.004$), real puncture lengths during and after training (AR and Post AR) were both shorter than before training (Pre AR). In addition, for the path ratio ($F(2,139)=25.014$, $p<0.0001$), equivalent ratios were obtained during and after training (AR and Post AR), and both were significantly lower than before training (Pre AR), indicating closer to ideal linear trajectories. Regarding the path difference metric, this reinforces the fact of having better trajectories during and after training because, again, similar differences during (AR) and after (Post AR) training were observed, and also both were significantly smaller than before the training (Pre AR) ($F(2,139)=10.51$, $p<0.0001$). No main effect was revealed for angle, but even if not significantly, similar angles of the executed trajectories were observed for AR and Post AR conditions, both smaller than Pre-AR. **Table 4** presents the complete descriptive statistics grouped by expert level, comparing the exhibited skills performance before and after the training with the augmented reality assistance.

	Task Condition			p-value
	Pre AR (n=18)	AR (n=18)	Post AR (n=18)	
Path Metrics				
Angle [°]	69.37±2.53	63.14±2.53	62.80±2.53	NS
Ideal Path Length [mm]	105.24±8.7	139.41±9.06	114.52±8.7	0.022 (F=3.92)
Path Length [mm]	208.95±129.84	174.47±74.52	147.97±69.95	0.004 (F=5.753)
Path Ratio	1.88±0.65	1.30±0.33	1.31±0.41	<0.0001 (F=25.014)
Path Difference [mm ²]	10.08±9.39	4.96±2.87	4.84±3.99	<0.0001 (F=10.51)
Target Error				
Coronal Plane (XY) [mm]	10.22±15.11	4.46±1.76	4.67±3.49	<0.0001 (F=10.73)

Traversal Plane (XZ) [mm]	20.29±15.73	1.49±1.88	4.98±5.92	<0.0001 (F=40.17)
Sagittal Plane (YZ) [mm]	16.85±14.51	5.06±1.65	5.64±4.37	<0.0001 (F=22.09)
Spatial [mm]	22.15±18.43	3.88±2.15	5.69±5.02	<0.0001 (F=34.52)

Table 3. Observed metrics of the ventricular puncture comparing the execution of the procedure by task condition, before, during, and after the training using the augmented reality visual assistance.

The boxplots in **Figure 13** show a graphical comparison of the spatial error, path length, path ratio, and path difference between the three task conditions. It evidences similarities between the training and post-training, with significant improvements of the former regarding before the training.

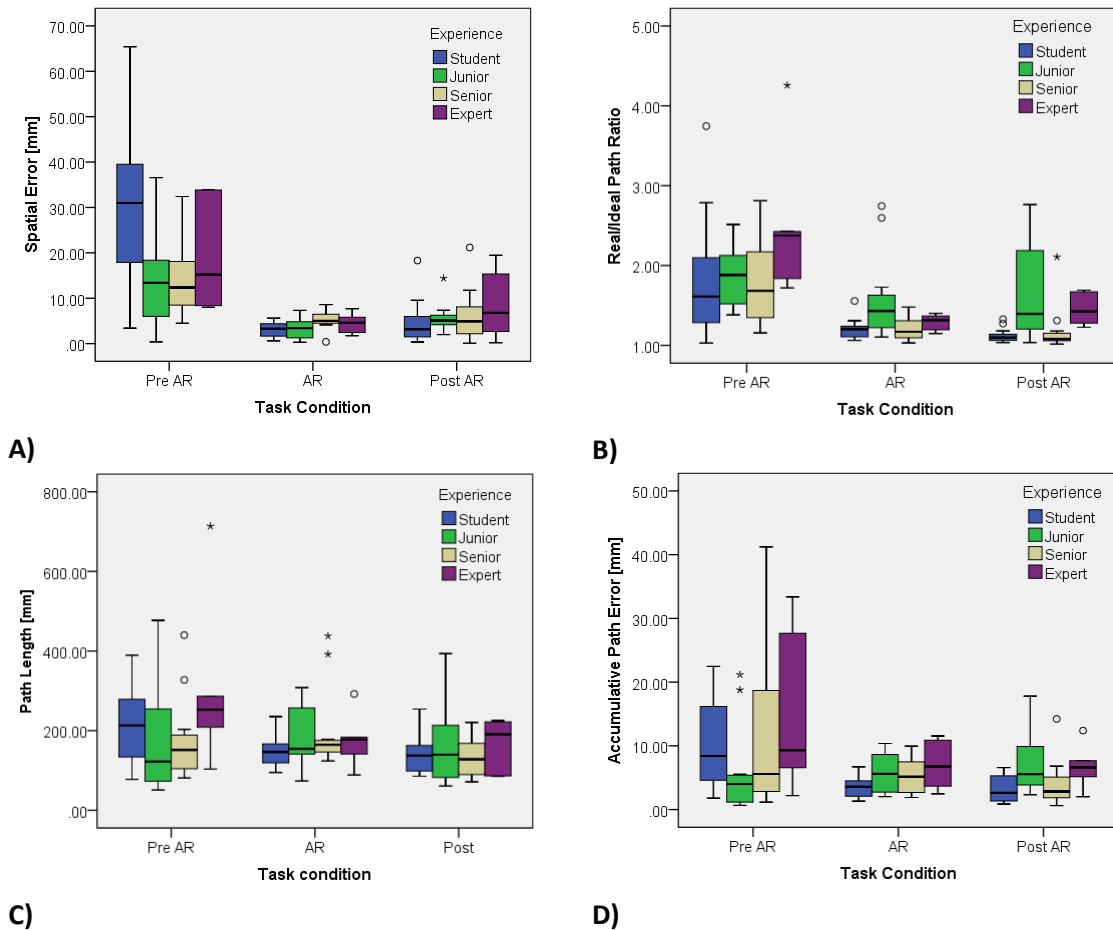


Figure 13. Boxplots showing the comparisons of the mean and standard deviation of observed metrics during the three experimental conditions. A) The achieved spatial error in reaching the target Monro foramen. B) The path ratio between the real executed trajectory concerning the ideal path trajectory, as an indicator of the curvature extent of the puncture. C) The path length from the starting to the ending points of the executed trajectories of the punctures. D) The difference between the real and ideal trajectory paths, computed as the accumulative error between both trajectories.

Table 5 reports the frequency distribution of errors of the participants, comparing the mean error computed over the punctures executed during the AR assistance and before and after the training. It can be observed that before the training, in around 45% of the punctures, the final position of the tip of the catheter ended farther than 20mm from the Monro foramen. With only about 13% within a distance of 5mm. On the other hand, around 68% of the punctures during the AR training achieved an error of up to 5mm, while 32% were within 5-10mm. After the training with AR, only around 2% of the punctures occurred farther than 20mm. Contrary, in about 68% of the punctures, the catheter tip was placed below 5mm to the target, and in around 32% between 5-10mm. Therefore, evidencing a substantial improvement in the number of correct punctures after training.

	Experience							
	Student (n=18)		Junior (n=11)		Senior (n=12)		Expert (n=5)	
	Pre AR	Post AR	Pre AR	Post AR	Pre AR	Post AR	Pre AR	Post AR
Path Metrics								
Angle [°]	61.27 ± 18.63	66.24 ± 8.28	65.64 ± 16.91	65.68 ± 12.26	70.01 ± 18.42	64.28 ± 14.29	80.58 ± 37.21	55.01 ± 13.42
Ideal Path Length [mm]	123.30 ± 31.39	129.26 ± 48.27	88.37 ± 56.90	109.76 ± 98.83	93.55 ± 43.92	114.15 ± 38.78	115.73 ± 37.69	104.91 ± 57.15
Path Length [mm]	221.39 ± 93.91	144.28 ± 55.0	176.97 ± 135.55	162.77 ± 105.99	176.29 ± 106.28	134.12 ± 52.58	312.94 ± 234.44	161.94 ± 70.85
Path Ratio	1.79 ± 0.69	1.12 ± 0.08	1.87 ± 0.41	1.68 ± 0.62	1.77 ± 0.51	1.18 ± 0.30	2.52 ± 1.02	1.46 ± 0.22
Path Difference [mm²]	10.06 ± 6.37	3.26 ± 2.11	6.12 ± 7.12	7.47 ± 5.33	11.37 ± 12.25	4.02 ± 3.74	15.82 ± 13.81	4.84 ± 3.99
Target Error								
Coronal Plane (XY) [mm]	9.15 ± 7.63	5.11 ± 4.01	9.25 ± 10.95	5.12 ± 4.23	5.13 ± 2.80	3.72 ± 2.53	25.41 ± 4.39	4.39 ± 2.06
Traversal Plane (XZ) [mm]	30.08 ±	4.17 ±	9.99 ±	2.96 ±	15.88 ±	6.20 ±	18.68 ±	8.63 ±

	17.61	3.41	8.53	2.97	11.06	8.53	13.47	8.62
Sagittal Plane (YZ)	24.98	4.71	8.38	5.76	11.61	6.18	18.54	7.09
[mm]	±	±	±	±	±	±	±	±
	14.40	3.41	10.21	3.38	9.31	5.61	19.21	6.11
Spatial	29.92	4.46	13.43	5.69	14.78	6.11	29.52	8.53
[mm]	±	±	±	±	±	±	±	±
	16.89	4.30	10.35	3.25	9.14	5.86	34.32	7.53

Table 4. The statistical descriptors of the observed metrics of the ventricular puncture were grouped by experience level, comparing the execution before and after the training using the augmented reality visual assistance.

Finally, an analysis of spatial puncture location within four puncture regions previously defined (right horn, left horn, right body, left body, and third ventricle), comparing the Pre-AR and Post-AR experimental conditions. **Figure 14** shows the division by regions of the ventricular system in the clinical case. In this analysis, three types of punctures could be identified. 1) The ideal puncture, which describes the positioning of the catheter tip within a 3-mm spherical region, corresponding to the position and diameter of the neck of the foramen of Monro. 2) The correct puncture, where the tip of the catheter is positioned within the right frontal horn of the ventricular system, and there is the outflow of cerebrospinal fluid. 3) The risk puncture, which identifies that the tip of the catheter is on the right body, left horn, left body, or outside the regions. **Figure 15** shows the distribution of punctures before and after assistance with augmented reality, showing more grouped punctures around the target point and with less error after practicing with AR.

Error [mm]	Pre [%]	AR [%]	Post [%]	Error [mm]	Pre [%]	AR [%]	Post [%]
0-2	2.13	25.53	23.40	<2	2.13	25.53	23.40
2-5	10.64	42.55	29.79	<5	12.77	68.08	53.19
5-10	19.15	31.91	34.04	<10	31.92	100	87.23
10-15	12.77	0	4.26	<15	44.69	100	91.49
15-20	10.64	0	6.38	<20	55.33	100	97.87
>20	44.68	0	2.13	>20	0	0	2.13

Table 5. The frequency distribution of the achieved accuracy of the performed punctures by the participants, before, during, and after the training under the augmented reality visual assistance.

Figure 16 shows a greater occurrence of safe punctures and a decrease in risky punctures after training. As shown in detail, the results in the Pre-AR puncture group show that 36% (17 neurosurgeons) punctured the third ventricle, and 41% (19 neurosurgeons) punctured the right horn. Of the third ventricle puncture group, 83% (5 neurosurgeons) performed an

ideal puncture, and 17% (1 neurosurgeon) performed a puncture outside the ventricle. Among 23% (11 neurosurgeons) of the punctures were located in the left horn, which indicates a risky puncture since the catheter is contralateral to the puncture site (perforation of the septum pellucidum).

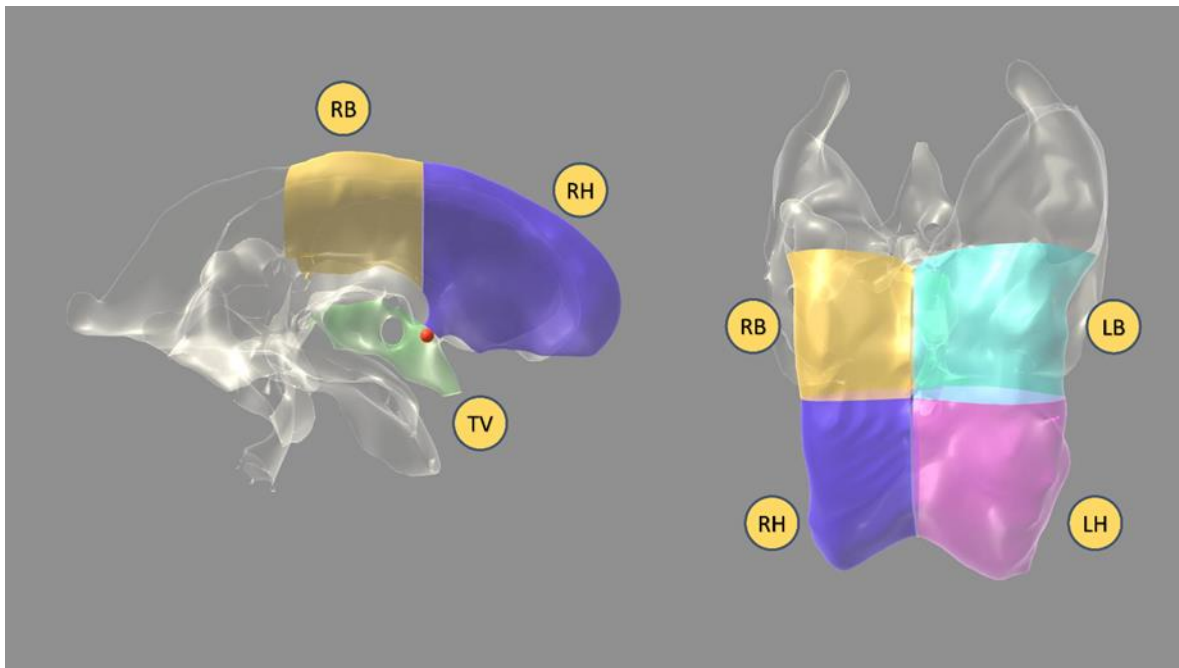


Figure 14. Spatial division by regions of the ventricular system describing the successful (TV: Third ventricle) and safe zone (RH: Right horn), versus risk (RB: Right ventricle body) and wrong locations (LH: Left horn, LB: Left ventricle body and any region outside the volume).

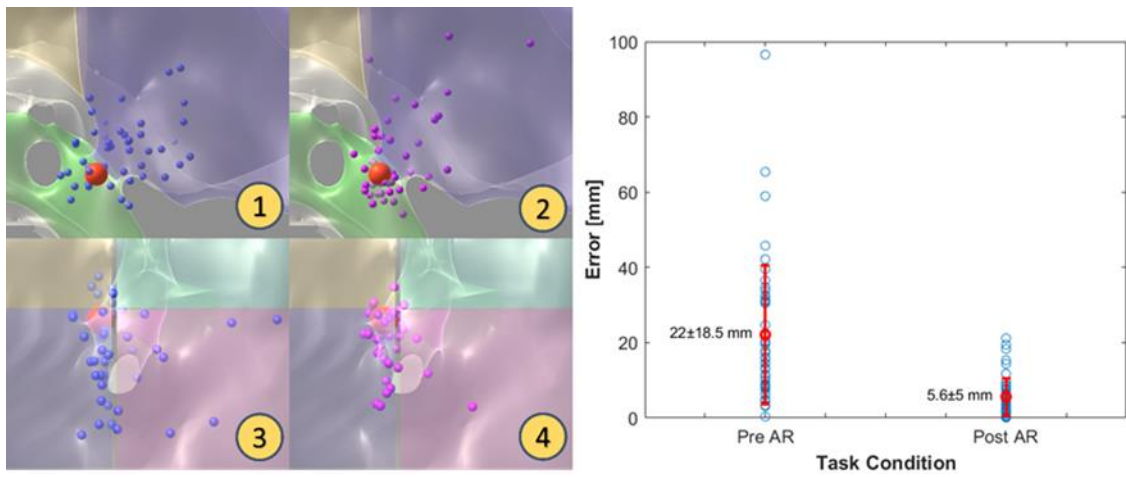


Figure 15. Spatial distribution of the ending locations of the catheter tip, comparing the PRE and POST punctures after the training under the augmented reality assistance. Left Above (1 - PRE, 2 – POST) are coronal views. Left Below (3 - PRE, 4 - POST) are axial views. Right, dispersion plot of error distribution comparing PRE and POST punctures, showing the mean and standard deviation of the errors.

Regarding the frequency of punctures in the Post-AR group, 57% (27 participants) of punctures on the third ventricle and 32% (15 participants) on the right horn were recorded. In the third ventricle puncture group, 92% (12 participants) of the punctures were identified as ideal, and 8% (1 participant) performed a puncture outside the ventricle. On the other hand, 9% of the trials (4 participants) resulted in a puncture in the left horn region. About 2% of the punctures (1 participant) placed the catheter in the left body.

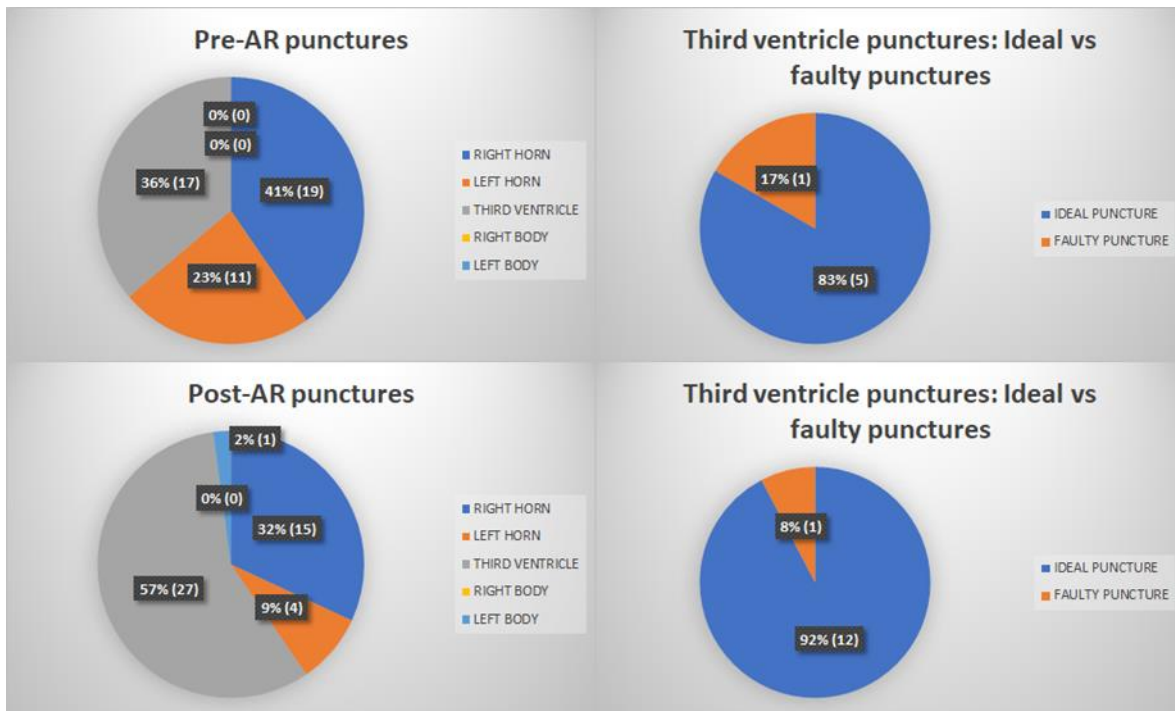


Figure 16. Frequency of the spatial distribution of the location of the catheter tip of the punctures, comparing before (Pre-AR) and after (Post-AR) the training with the augmented reality system Left) The location distribution within the four defined regions of interest within the ventricle. Right) The comparison between the correct (ideal) versus incorrect (faulty) punctures within the Third ventricle zone.

CHAPTER 7

DISCUSSION

Ventriculostomy is among the most performed procedures in neurosurgery. It is commonly performed by experienced residents. It is one of the first interventions learned by residents in their first years of training in residency programs. The prevalence of complications due to mislocated punctures in inadequate anatomical positions is relatively common, which can be more critical for inexperienced residents, increasing the risk of complications during catheter insertion. Reaffirming what was commented by (Schneider et al., 2021), the significant rate of puncture errors in ventriculostomy procedures can influence a poor prognosis for the patient after surgery.

Although the use of navigation systems can improve precision, thus reducing risk, in practice, it is often preferred to do it by free hand without using neuronavigation to avoid a work overload of more than a few minutes (Huyette et al., 2008; Sarrafzadeh et al., 2014; Schneider et al., 2021).

On the other hand, the interest in incorporating augmented reality into navigation has been growing in recent years (Stengel et al., 2022). Some studies using patient models with phantoms reported enhancements in accuracy during ventriculostomy procedures using augmented reality navigation setups (Hooten et al., 2014; Schneider et al., 2021). In particular, a study using Microsoft HoloLens (Schneider et al., 2021) showed an overall ventriculostomy success rate of 68% when using a vision-see-through augmented reality setup (VST). An enhancement in spatial accuracy of approximately 5 mm was observed for positive punctures compared to the accuracy of about 11mm for the resting 32% of unsuccessful (negative) punctures. In this case, three-dimensional visual augmentation was

projected towards a transversal plane from the participant's point of view, looking directly at the phantom. In our experiments, we achieved a remarkable enhancement in locating the target position at the Monro foramen during the visual augmentation. The augmented reality system achieved an overall spatial accuracy of around 3.88mm. Considerably less than the accuracy of 22mm obtained in the first punctures free-hand performed before the visual augmentation. In our case, the visual augmentation was presented in the sagittal plane projected over the phantom head, with the participants looking at the scene towards the monitor screen. In any case, our observed accuracy is in line with similar studies like the above. Interestingly, comparing the positioning errors concerning the projection of the target position in the coronal, sagittal, and traversal planes, a notorious enhancement in the three planes was evident when using augmented reality compared to the first free-hand punctures. Such enhancement is attributed to the manual orientation of the catheter before the insertion, given the anatomical landmarks of the patient model, plus the visual assistance even though this is provided only two-dimensionally in a sagittal plane.

A remarkable finding in our experiments is that after the training, almost 90% of the punctures relied on between 10mm from the target position, with half of them between 5mm. On the contrary, approximately half of the free hand punctures relied far from 20mm. Consequently, the risky punctures were drastically reduced after the training, with only one practitioner placing the catheter on the contralateral side farther from the anatomical medial reference plane. Complementary, the observed metrics regarding the quality of the performed trajectories with respect to the ideal reference trajectories, such as path length, path ratio, and path difference between the real and ideal trajectories, revealed significant enhancement after the training session with respect to the first free-hand punctures without the augmented reality assistance. This is an essential aspect because residents must learn to execute the puncture following the ideal safe trajectory for avoiding lesions in vital functional zones within the brain tissue.

Comparing the observed errors during the system calibration and training phases, it was found that the tracking error was about 0.86 mm in the calibration phase and about 1.13 mm with the anatomical landmarks on the skull model. On the other hand, the localization

error of the foramen of Monro during training with the AR guidance was 4 mm. Therefore, it can be argued that the error of the AR system does not directly impact the errors generated by the participants. Thus, it can be concluded that the observed errors are attributable to the execution of the puncture tasks and are reliable in the three experimental phases.

From the above, we can deduce that there is enough evidence of the feasibility of the proposed approach to be used as a valuable instrument for educating residents in neurosurgery. The proposed model can be introduced in the first stages of the residency to aid neurosurgery students with limited experience in acquiring enough skills safely before their first experiences with patients. Even experienced neurosurgeons could benefit as means for continuous training and reinforcement of dexterities.

This gives rise to future work, where the progress of the participants with different levels of experience can be measured in hours of training. In addition, as it is a computational simulation model, it also has the capacity to load different cases, which favors studying well-established ones and those complexes related to cranial deformations or brain malformations. Another possible advantage implies that a puncture can be approached from different cranial regions, depending on the clinical case. It would be possible to elaborate different computational 3D models from several clinical cases, with varying target sites to be reached from diverse access points. As a generalization, it is important to remember that ventricular puncture aims to reach and correctly position the catheter over an established region, passing through an entry point where it is crucial to have visual information about the work environment.

When carrying out the experiments with the navigator, only the puncture stage was considered, where it is assumed that the burr hole was previously performed and correctly located. However, it is important to evaluate in a subsequent study the effect of catheter placement where the burr hole was incorrect, as well as different punctures and entry regions since the literature (Kim et al., 2022) mentions that a ventriculostomy can be performed from different cranial regions. This consideration will help us to understand if the location of the burr hole influences the poor placement of the catheter. On the other

hand, interest has arisen in observing how the location of a burr hole affects the puncture and improving the system in such a way that it helps the neurosurgeon to correct the puncture. Another aspect to consider is the designation of the burr hole site and the reference guidelines by the user, considering pathologies related to obstructions due to tumors and cranial, cerebral, and ventricular malformations.

In this study, a single clinical case was adopted. However, it is important to homogenize the study by expanding the number of CT scans. Evaluating the position of the catheter tip and confirming that it is in the correct place, taking into account different pathologies, will generate more reliable data. Designing experiments where clinical cases are randomized may be helpful to counterbalance any possible bias due to adaptation to the presented single case.

In another aspect, it should be noted that there is high variability discernible in the participants' group for this study. One of the variables that we considered for the analysis of the data obtained was the experience level of each one of the participants; this is because we experimented only in a teaching hospital, whose academic staff for the subspecialty is less than that of the students.

Regarding the observed metrics of experts, we were surprised that their accuracy was worse than the observed in less experienced participants in general. This finding may be due to the limitation of our study in terms of the few expert participants, which could generate bias that would be reduced by incorporating more experts in subsequent studies. Another explanation is that some experts were deans who currently carry out academic and teaching duties. However, they no longer perform ventriculostomies, which could be reflected in their performance. If this were the case, then this reinforces the motivation for these kinds of training approaches to be applied on an ongoing basis as a lifetime task for surgeons of any grade of experience.

Thanks to collaborations with other hospitals and the impact of our study, we are expanding our work in a follow-up study, analyzing multiple grouping criteria and individual groups over time.

Another aspect of the study that must be considered is the waiting interval between the Pre-AR, AR, and Post-AR conditions. During the participation of each of the neurosurgeons, there was a waiting time between 60 and 120 seconds due to the saving of data once the user indicated the end of each stage. Taking into account that each doctor had a variation in execution time, this situation can be extrapolated to the waiting time for data to be dumped into a file. One of the questions that arise through this aspect is how the waiting time can influence the retention of learning generated through augmented reality. Once the data has been analyzed and based on the distribution of the points in **Figure 15** and the percentages in **Figure 16**, an improvement in catheter positioning and the relationship with the percentages according to the ventricular regions can be noted. However, the question arises about how these data would behave if the waiting times were longer. In fact, as well as studying other factors, such as increasing the duration and number of practices over time, even in days, compared with traditional training without AR guidance. For this reason, a subsequent study must be conducted following a new experimental design, including study control groups, varying waiting times, more extended periods, and repeated practicing sessions, to understand how these factors may influence the enhancement of positioning catheters.

During the development of the navigator, all interaction models are considered rigid. This feature allows us to record the virtual models to the physical ones. It is important to explore the influence of semi-flexible and flexible tools to make the simulation even more realistic. Favorably, there is already research regarding the registration of deformable models where both optical and electromagnetic registration techniques are applied. Based on the aforementioned (Ferrari et al., 2016), incorporating these new approaches into simulation systems will increase the fidelity of current systems since such flexible models could be applied to tissues such as skin, veins, and arteries as brain parenchyma.

On the other hand, exploring the influence of haptic feedback as an additional indicator for the correct execution of a surgical task may yield more realistic experience and performance data from those currently obtained. Besides, incorporating the haptic feedback would limit the advance and retreat maneuvers of the catheter as it occurs in reality due to

the brain's soft tissue. Despite the technical limitations previously discussed, such as the automation in the analysis of data from the simulations, the variety of clinical cases, the incorporation of haptic feedback, the replication of materials, or the use of real tools adapted to the system, we consider our results valuable to show the importance and feasibility of augmented reality models for training and even the design of new and simpler navigation tools in the scope of ventriculostomy procedures.

As future work, it is planned to include a head-mounted display and a stereoscopic view of the environment. Simulation with augmented reality can be studied to enable freedom of movement and compare the simulation from different visual perspectives. In addition, it must be considered that a tactile sensation is transmitted through the tool during the puncture. This generates the curiosity of how a tactile interaction influences the results already obtained, probably by incorporating a haptic feedback device or physical phantom mimicking the brain tissue.

Finally, the present study reinforces the motivation for designing compact navigation schemes specifically designed for ventriculostomy in the near future. However, more efforts must be made to migrate the augmented reality navigation setups from test environments using phantoms to clinical scenarios with patients.

CHAPTER 8

CONCLUSION

This document presents a screen-based augmented reality system for training ventricular puncture procedures. It displays a projection of visual information such as virtual 3D anatomies of the ventricles over a 3D printed patient model obtained from a CT image studio. The results of the experimental study confirm that regardless of the level of

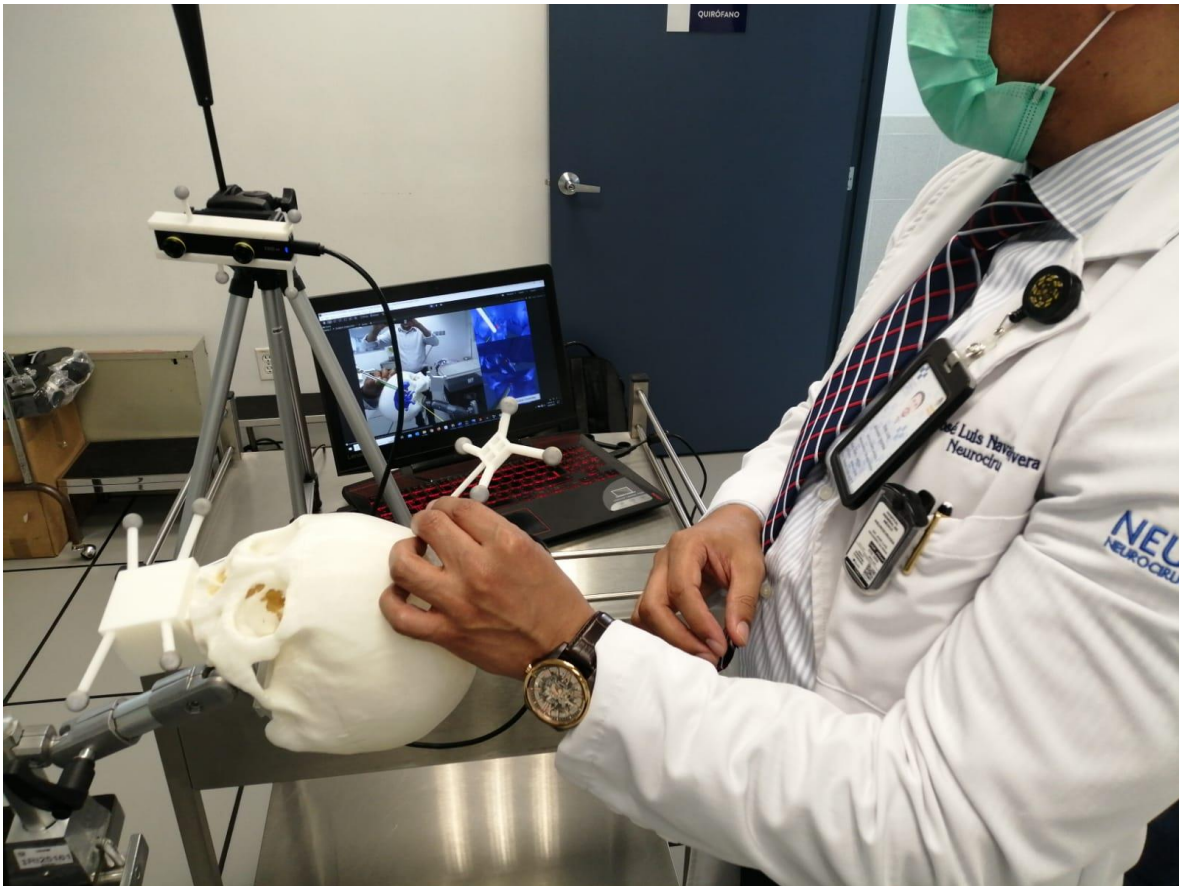


Figure 17. Expert neurosurgeon, performing a series of punctures prior to a course proposal with our navigator at the General Hospital of Mexico "Dr. Eduardo Liceaga".

experience, most participants, even novice practitioners, enhance their accuracy in reaching the Monro foramen during the AR guidance. Moreover, other metrics related to the morphology of the executed trajectories of the punctures reveal an improvement in the execution skills after the training in general for all participants, including experienced practitioners. It confirms the feasibility of AR as a training tool and motivates the development of future studies toward the standardization of new educative methodologies in neurosurgery. As a result of the work carried out (Domínguez-Velasco et al., 2023), the navigator has been made available to the Center for Improvement and Medical Skills of the General Hospital of Mexico "Dr. Eduardo Liceaga" for its use in training and simulating the ventricular puncture procedure for neurosurgeons of the four categories evaluated. **Figure 17** shows the assembled and functional navigator.

BIBLIOGRAPHY

- Alaraj, A., Luciano, C. J., Bailey, D. P., Elsenousi, A., Roitberg, B. Z., Bernardo, A., Banerjee, P. P., & Charbel, F. T. (2015). Virtual Reality Cerebral Aneurysm Clipping Simulation With Real-Time Haptic Feedback. *Operative Neurosurgery*, *11*(1), 52–58.
<https://doi.org/10.1227/NEU.0000000000000583>
- AlZhrani, G., Alotaibi, F., Azarnoush, H., Winkler-Schwartz, A., Sabbagh, A., Bajunaid, K., Lajoie, S. P., & Del Maestro, R. F. (2015). Proficiency Performance Benchmarks for Removal of Simulated Brain Tumors Using a Virtual Reality Simulator NeuroTouch. *Journal of Surgical Education*, *72*(4), 685–696. <https://doi.org/10.1016/j.jsurg.2014.12.014>
- Arun, K. S., Huang, T. S., & Blostein, S. D. (1987). Least-Squares Fitting of Two 3-D Point Sets. *IEEE Transactions on Pattern Analysis and Machine Intelligence*, *PAMI-9*(5), 698–700.
<https://doi.org/10.1109/TPAMI.1987.4767965>
- Ayoub, A., & Pulijala, Y. (2019). The application of virtual reality and augmented reality in Oral & Maxillofacial Surgery. *BMC Oral Health*, *19*(1), 238. <https://doi.org/10.1186/s12903-019-0937-8>
- Bagher Zadeh Ansari, N., Léger, É., & Kersten-Oertel, M. (2022). VentroAR: An augmented reality platform for ventriculostomy using the Microsoft HoloLens. *Computer Methods in Biomechanics and Biomedical Engineering: Imaging & Visualization*, 1–9.
<https://doi.org/10.1080/21681163.2022.2156394>

- Baum, Z. M. C., Lasso, A., Ryan, S., Ungi, T., Rae, E., Zevin, B., Levy, R., & Fichtinger, G. (2019). Augmented Reality Training Platform for Neurosurgical Burr Hole Localization. *Journal of Medical Robotics Research*, *04*(03n04), 1942001.
<https://doi.org/10.1142/S2424905X19420017>
- Belykh, E., & Byvaltsev, V. (2014). Off-the-Job Microsurgical Training on Dry Models: Siberian Experience. *World Neurosurgery*, *82*(1), 20–24.
<https://doi.org/10.1016/j.wneu.2014.01.018>
- Cabrilo, I., Bijlenga, P., & Schaller, K. (2014). Augmented Reality in the Surgery of Cerebral Aneurysms: A Technical Report. *Operative Neurosurgery*, *10*(2), 252–261.
<https://doi.org/10.1227/NEU.0000000000000328>
- Choque-Velasquez, J., Colasanti, R., Collan, J., Kinnunen, R., Rezai Jahromi, B., & Hernesniemi, J. (2018). Virtual Reality Glasses and “Eye-Hands Blind Technique” for Microsurgical Training in Neurosurgery. *World Neurosurgery*, *112*, 126–130.
<https://doi.org/10.1016/j.wneu.2018.01.067>
- Contreras López, W. O., Navarro, P. A., & Crispin, S. (2019). Intraoperative clinical application of augmented reality in neurosurgery: A systematic review. *Clinical Neurology and Neurosurgery*, *177*, 6–11. <https://doi.org/10.1016/j.clineuro.2018.11.018>
- Cutolo, F., Meola, A., Carbone, M., Sinceri, S., Cagnazzo, F., Denaro, E., Esposito, N., Ferrari, M., & Ferrari, V. (2017). A new head-mounted display-based augmented reality system in neurosurgical oncology: A study on phantom. *Computer Assisted Surgery*, *22*(1), 39–53.
<https://doi.org/10.1080/24699322.2017.1358400>

- De Paolis, L. T., & De Luca, V. (2019). Augmented visualization with depth perception cues to improve the surgeon's performance in minimally invasive surgery. *Medical & Biological Engineering & Computing*, 57(5), 995–1013. <https://doi.org/10.1007/s11517-018-1929-6>
- De Paolis, L. T., & Ricciardi, F. (2018). Augmented visualisation in the treatment of the liver tumours with radiofrequency ablation. *Computer Methods in Biomechanics and Biomedical Engineering: Imaging & Visualization*, 6(4), 396–404. <https://doi.org/10.1080/21681163.2017.1287598>
- De Paolis, L. T., Vite, S. T., Castañeda, M. Á. P., Domínguez Velasco, C. F., Muscatello, S., & Hernández Valencia, A. F. (2022). An Augmented Reality Platform with Hand Gestures-Based Navigation for Applications in Image-Guided Surgery: Prospective Concept Evaluation by Surgeons. *International Journal of Human-Computer Interaction*, 38(2), 131–143. <https://doi.org/10.1080/10447318.2021.1926116>
- Delorme, S., Laroche, D., DiRaddo, R., & F. Del Maestro, R. (2012). NeuroTouch: A Physics-Based Virtual Simulator for Cranial Microneurosurgery Training. *Operative Neurosurgery*, 71, ons32–ons42. <https://doi.org/10.1227/NEU.0b013e318249c744>
- Desselle, M. R., Brown, R. A., James, A. R., Midwinter, M. J., Powell, S. K., & Woodruff, M. A. (2020). Augmented and Virtual Reality in Surgery. *Computing in Science Engineering*, 22(3), 18–26. <https://doi.org/10.1109/MCSE.2020.2972822>
- Domínguez-Velasco, C. F., Tello-Mata, I. E., Guinto-Nishimura, G., Martínez-Hernández, A., Alcocer-Barradas, V., Pérez-Lomelí, J. S., & Padilla-Castañeda, M. A. (2023). Augmented reality simulation as training model of ventricular puncture: Evidence in the improvement of the quality of punctures. *The International Journal of Medical Robotics and Computer Assisted Surgery*, e2529. <https://doi.org/10.1002/rcs.2529>

- Dubin, A. K., Smith, R., Julian, D., Tanaka, A., & Mattingly, P. (2017). A Comparison of Robotic Simulation Performance on Basic Virtual Reality Skills: Simulator Subjective Versus Objective Assessment Tools. *Journal of Minimally Invasive Gynecology*, *24*(7), 1184–1189. <https://doi.org/10.1016/j.jmig.2017.07.019>
- Eagleson, R., & Ribaupierre, S. D. (2018). Visual Perception and Human–Computer Interaction in Surgical Augmented and Virtual Reality Environments. In T. M. Peters, C. A. Linte, Z. Yaniv, & J. Williams (Eds.), *Mixed and Augmented Reality in Medicine* (1st ed., pp. 83–98). CRC Press. <https://doi.org/10.1201/9781315157702-6>
- Ecke, U., Luebben, B., Maurer, J., Boor, S., & Mann, W. (2003). Comparison of Different Computer-Aided Surgery Systems in Skull Base Surgery. *Skull Base*, *13*(01), 043–050. <https://doi.org/10.1055/s-2003-37552>
- Ericsson, K. A. (2004). Deliberate Practice and the Acquisition and Maintenance of Expert Performance in Medicine and Related Domains. *Academic Medicine*, *79*(10), S70.
- Fedorov, A., Beichel, R., Kalpathy-Cramer, J., Finet, J., Fillion-Robin, J.-C., Pujol, S., Bauer, C., Jennings, D., Fennessy, F., Sonka, M., Buatti, J., Aylward, S., Miller, J. V., Pieper, S., & Kikinis, R. (2012). 3D Slicer as an image computing platform for the Quantitative Imaging Network. *Magnetic Resonance Imaging*, *30*(9), 1323–1341. <https://doi.org/10.1016/j.mri.2012.05.001>
- Ferrari, V., Vigliani, R. M., Nicoli, P., Cutolo, F., Condino, S., Carbone, M., Siesto, M., & Ferrari, M. (2016). Augmented reality visualization of deformable tubular structures for surgical simulation: SimARdeformable. *The International Journal of Medical Robotics and Computer Assisted Surgery*, *12*(2), 231–240. <https://doi.org/10.1002/rcs.1681>

- Fetić, A., Jurić, D., & Osmanović, D. (2012). The procedure of a camera calibration using Camera Calibration Toolbox for MATLAB. *2012 Proceedings of the 35th International Convention MIPRO*, 1752–1757.
- Fiani, B., De Stefano, F., Kondilis, A., Covarrubias, C., Reier, L., & Sarhadi, K. (2020). Virtual Reality in Neurosurgery: “Can You See It?”—A Review of the Current Applications and Future Potential. *World Neurosurgery*, *141*, 291–298.
<https://doi.org/10.1016/j.wneu.2020.06.066>
- Ganguli, A., Pagan-Diaz, G. J., Grant, L., Cvetkovic, C., Bramlet, M., Vozenilek, J., Kesavadas, T., & Bashir, R. (2018). 3D printing for preoperative planning and surgical training: A review. *Biomedical Microdevices*, *20*(3), 65. <https://doi.org/10.1007/s10544-018-0301-9>
- García Navarro, V., & Castillo Velázquez, G. (2016). Estrategias y abordajes en neurocirugía craneal. *Amolca. México DF*.
- Gilbert, J. W., Wheeler, G. R., Spitalieri, J. R., & Mick, G. E. (2009). Ventriculostomy Catheter Placement. *Journal of Neurosurgery*, *110*(1), 193–195.
<https://doi.org/10.3171/JNS.2009.110.1.0193a>
- Gmeiner, M., Dirnberger, J., Fenz, W., Gollwitzer, M., Wurm, G., Trenkler, J., & Gruber, A. (2018). Virtual Cerebral Aneurysm Clipping with Real-Time Haptic Force Feedback in Neurosurgical Education. *World Neurosurgery*, *112*, e313–e323.
<https://doi.org/10.1016/j.wneu.2018.01.042>
- Goo, H. W., Park, S. J., & Yoo, S.-J. (2020). Advanced Medical Use of Three-Dimensional Imaging in Congenital Heart Disease: Augmented Reality, Mixed Reality, Virtual Reality, and Three-Dimensional Printing. *Korean Journal of Radiology*, *21*(2), 133.
<https://doi.org/10.3348/kjr.2019.0625>

- Gray, H., Standring, S., & Anhand, N. (Eds.). (2021). *Gray's Anatomy: The anatomical basis of clinical practice* (42nd edition). Elsevier.
- Hess, R. (2010). An Introduction to 3DRecreating the World Inside Your Computer, or Not. In *Blender Foundations* (pp. 1–11). Elsevier. <https://doi.org/10.1016/B978-0-240-81430-8.00001-9>
- Hooten, K. G., Lister, J. R., Lombard, G., Lizdas, D. E., Lampotang, S., Rajon, D. A., Bova, F., & Murad, G. J. A. (2014). Mixed Reality Ventriculostomy Simulation: Experience in Neurosurgical Residency. *Operative Neurosurgery*, *10*(4), 565–576. <https://doi.org/10.1227/NEU.0000000000000503>
- Horaud, R., & Dornaika, F. (1995). Hand-Eye Calibration. *The International Journal of Robotics Research*, *14*(3), 195–210. <https://doi.org/10.1177/027836499501400301>
- Huang, T., Yang, C., Hsieh, Y., Wang, J., & Hung, C. (2018). Augmented reality (AR) and virtual reality (VR) applied in dentistry. *The Kaohsiung Journal of Medical Sciences*, *34*(4), 243–248. <https://doi.org/10.1016/j.kjms.2018.01.009>
- Huyette, D. R., Turnbow, B. J., Kaufman, C., Vaslow, D. F., Whiting, B. B., & Oh, M. Y. (2008). Accuracy of the freehand pass technique for ventriculostomy catheter placement: Retrospective assessment using computed tomography scans. *Journal of Neurosurgery*, *108*(1), 88–91. <https://doi.org/10.3171/JNS/2008/108/01/0088>
- Hvolbek, A. P., Nilsson, P. M., Sanguedolce, F., & Lund, L. (2019). A prospective study of the effect of video games on robotic surgery skills using the high-fidelity virtual reality RobotiX simulator. *Advances in Medical Education and Practice*, *10*, 627–634. <https://doi.org/10.2147/AMEP.S199323>

- Jud, L., Fotouhi, J., Andronic, O., Aichmair, A., Osgood, G., Navab, N., & Farshad, M. (2020). Applicability of augmented reality in orthopedic surgery – A systematic review. *BMC Musculoskeletal Disorders*, *21*(1), 103. <https://doi.org/10.1186/s12891-020-3110-2>
- Kashikar, T. S., Kerwin, T. F., Moberly, A. C., & Wiet, G. J. (2019). A review of simulation applications in temporal bone surgery. *Laryngoscope Investigative Otolaryngology*, *4*(4), 420–424. <https://doi.org/10.1002/lio2.277>
- Kersten-Oertel, M., Gerard, I., Drouin, S., Mok, K., Sirhan, D., Sinclair, D. S., & Collins, D. L. (2015). Augmented reality in neurovascular surgery: Feasibility and first uses in the operating room. *International Journal of Computer Assisted Radiology and Surgery*, *10*(11), 1823–1836. <https://doi.org/10.1007/s11548-015-1163-8>
- Kim, J., Kim, J. H., Lee, W., Han, H. J., Park, K. Y., Chung, J., Kim, Y. B., Joo, J. Y., & Park, S. K. (2022). Predictors of Ventriculostomy-Associated Infections: A Retrospective Study of 243 Patients. *World Neurosurgery*, *160*, e40–e48. <https://doi.org/10.1016/j.wneu.2021.12.085>
- Lai, M., Shan, C., & With, P. (2018). *Hand-Eye Camera Calibration with an Optical Tracking System*. 1–6. <https://doi.org/10.1145/3243394.3243700>
- Loh, C. Y. Y., Wang, A. Y. L., Tiong, V. T. Y., Athanassopoulos, T., Loh, M., Lim, P., & Kao, H.-K. (2018). Animal models in plastic and reconstructive surgery simulation—A review. *Journal of Surgical Research*, *221*, 232–245. <https://doi.org/10.1016/j.jss.2017.08.052>
- Meola, A., Cutolo, F., Carbone, M., Cagnazzo, F., Ferrari, M., & Ferrari, V. (2017). Augmented reality in neurosurgery: A systematic review. *Neurosurgical Review*, *40*(4), 537–548. <https://doi.org/10.1007/s10143-016-0732-9>

- Mostofi, K., & Khouzani, R. (2016). Surface anatomy for implantation of external ventricular drainage: Some surgical remarks. *Surgical Neurology International*, 7(23), 577.
<https://doi.org/10.4103/2152-7806.189437>
- Muralidharan, R. (2015). External ventricular drains: Management and complications. *Surgical Neurology International*, 6(7), 271. <https://doi.org/10.4103/2152-7806.157620>
- Neurosurgical Atlas. (2023). *Standard procedure of external ventricular drain (EVD) placement*.
https://assets.neurosurgicalatlas.com/volumes/ATLAS/1-PRINCIPLES_OF_CRANIAL_SURGERY/16-External_Ventricular_Drain/PCS_ExtIntraventDrain_03.jpg
- Park, F. C., & Martin, B. J. (1994). Robot sensor calibration: Solving $AX=XB$ on the Euclidean group. *IEEE Transactions on Robotics and Automation*, 10(5), 717–721.
<https://doi.org/10.1109/70.326576>
- Persky, S., & Lewis, M. A. (2019). Advancing science and practice using immersive virtual reality: What behavioral medicine has to offer. *Translational Behavioral Medicine*, 9(6), 1040–1046. <https://doi.org/10.1093/tbm/ibz068>
- Redberg, R. F. (2009). Cancer Risks and Radiation Exposure From Computed Tomographic Scans: How Can We Be Sure That the Benefits Outweigh the Risks? *Archives of Internal Medicine*, 169(22), 2049. <https://doi.org/10.1001/archinternmed.2009.453>
- Sarrafzadeh, A., Smoll, N., & Schaller, K. (2014). Guided (VENTRI-GUIDE) versus freehand ventriculostomy: Study protocol for a randomized controlled trial. *Trials*, 15(1), 478.
<https://doi.org/10.1186/1745-6215-15-478>

- Schirmer, C. M., Elder, J. B., Roitberg, B., & Lobel, D. A. (2013). Virtual Reality–Based Simulation Training for Ventriculostomy: An Evidence-Based Approach. *Neurosurgery*, 73(supplement 1), S66–S73. <https://doi.org/10.1227/NEU.0000000000000074>
- Schneider, M., Kunz, C., Pal’a, A., Wirtz, C. R., Mathis-Ullrich, F., & Hlaváč, M. (2021). Augmented reality–assisted ventriculostomy. *Neurosurgical Focus*, 50(1), E16.
- Stengel, F. C., Gandia-Gonzalez, M. L., Aldea, C. C., Bartek, J., Belo, D., Ben-Shalom, N., De La Cerda-Vargas, M. F., Drosos, E., Freyschlag, C. F., Kaprovoy, S., Lepic, M., Lippa, L., Rabiei, K., Raffa, G., Sandoval-Bonilla, B. A., Schwake, M., Spiriev, T., Zoia, C., & Stienen, M. N. (2022). Transformation of neurosurgical training from “see one, do one, teach one” to AR/VR & simulation – A survey by the EANS Young Neurosurgeons. *Brain and Spine*, 2, 100929. <https://doi.org/10.1016/j.bas.2022.100929>
- Subramonian, K., & Muir, G. (2004). The “learning curve” in surgery: What is it, how do we measure it and can we influence it? *BJU International*, 93(9), 1173–1174. <https://doi.org/10.1111/j.1464-410X.2004.04891.x>
- Teodoro-Vite, S., Pérez-Lomelí, J. S., Domínguez-Velasco, C. F., Hernández-Valencia, A. F., Capurso-García, M. A., & Padilla-Castañeda, M. A. (2021). A High-Fidelity Hybrid Virtual Reality Simulator of Aneurysm Clipping Repair With Brain Sylvian Fissure Exploration for Vascular Neurosurgery Training. *Simulation in Healthcare: The Journal of the Society for Simulation in Healthcare*, 16(4), 285–294. <https://doi.org/10.1097/SIH.0000000000000489>
- Toma, A. K., Camp, S., Watkins, L. D., Grieve, J., & Kitchen, N. D. (2009). EXTERNAL VENTRICULAR DRAIN INSERTION ACCURACY. *Neurosurgery*, 65(6), 1197–1201. <https://doi.org/10.1227/01.NEU.0000356973.39913.0B>

- Tuceryan, M., Greer, D. S., Whitaker, R. T., Breen, D. E., Crampton, C., Rose, E., & Ahlers, K. H. (1995). Calibration requirements and procedures for a monitor-based augmented reality system. *IEEE Transactions on Visualization and Computer Graphics*, 1(3), 255–273. <https://doi.org/10.1109/2945.466720>
- Unity®. (2023). [Computer software]. Unity Technologies. unity.com
- Vávra, P., Roman, J., Zonča, P., Ihnát, P., Němec, M., Kumar, J., Habib, N., & El-Gendi, A. (2017). Recent Development of Augmented Reality in Surgery: A Review. *Journal of Healthcare Engineering*, 2017, 1–9. <https://doi.org/10.1155/2017/4574172>
- Wei, Kumsok Kang, Huamin Yang, Yu Miao, Weili Shi, Fei He, Fei Yan, Zhengang Jiang, & Huimao Zhang. (2015). A hand-eye calibration method for computer assisted endoscopy. *2015 11th International Conference on Natural Computation (ICNC)*, 850–855. <https://doi.org/10.1109/ICNC.2015.7378102>
- Yudkowsky, R., Luciano, C., Banerjee, P., Schwartz, A., Alaraj, A., Lemole, G. M., Charbel, F., Smith, K., Rizzi, S., Byrne, R., Bendok, B., & Frim, D. (2013). Practice on an augmented reality/haptic simulator and library of virtual brains improves residents' ability to perform a ventriculostomy. *Simulation in Healthcare: Journal of the Society for Simulation in Healthcare*, 8(1), 25–31. <https://doi.org/10.1097/SIH.0b013e3182662c69>
- Zhalmukhamedov, E., & Urakov, T. M. (n.d.). *Current and future use of virtual and augmented reality in neurosurgery: A literature review*. 5.
- Zhang, Z. (2000). A flexible new technique for camera calibration. *IEEE Transactions on Pattern Analysis and Machine Intelligence*, 22(11), 1330–1334. <https://doi.org/10.1109/34.888718>